

12

MISCELLANEOUS PAPER GL-84-20

# PREDICTED AND ACTUAL PERFORMANCE OF A STRUCTURE IN EXPANSIVE SOILS

by

Mark E. Simmons

Foundations and Materials Branch  
US Army Engineer District, Fort Worth  
Fort Worth, Texas 76102

AD-A149 669



November 1984  
Final Report

Approved For Public Release; Distribution Unlimited

**DTIC**  
**ELECTE**  
JAN 30 1985  
**S** **D**  
**B**

DTIC FILE COPY

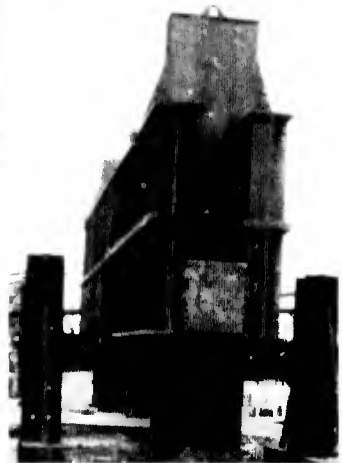
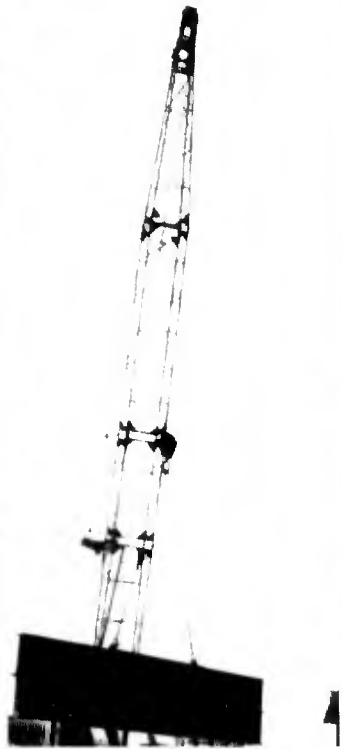
Prepared for DEPARTMENT OF THE ARMY  
US Army Corps of Engineers  
Washington, DC 20314-1000

Monitored by Geotechnical Laboratory  
US Army Engineer Waterways Experiment Station  
PO Box 631, Vicksburg, Mississippi 39180-0631

85 01 22 017



US Army Corps  
of Engineers



Destroy this report when no longer needed. Do not return  
it to the originator.

The findings in this report are not to be construed as an official  
Department of the Army position unless so designated  
by other authorized documents.

The contents of this report are not to be used for  
advertising, publication, or promotional purposes.  
Citation of trade names does not constitute an  
official endorsement or approval of the use of  
such commercial products.

Unclassified

SECURITY CLASSIFICATION OF THIS PAGE (When Data Entered)

REPORT DOCUMENTATION PAGE		READ INSTRUCTIONS BEFORE COMPLETING FORM
1. REPORT NUMBER Miscellaneous Paper GL-84-20	2. GOVT ACCESSION NO.	3. RECIPIENT'S CATALOG NUMBER
4. TITLE (and Subtitle) PREDICTED AND ACTUAL PERFORMANCE OF A STRUCTURE IN EXPANSIVE SOILS	5. TYPE OF REPORT & PERIOD COVERED Final report	
	6. PERFORMING ORG. REPORT NUMBER	
7. AUTHOR(s) Mark E. Simmons	8. CONTRACT OR GRANT NUMBER(s)	
9. PERFORMING ORGANIZATION NAME AND ADDRESS US Army Engineer District, Fort Worth Foundations and Materials Branch Fort Worth, Texas 76102	10. PROGRAM ELEMENT, PROJECT, TASK AREA & WORK UNIT NUMBERS	
11. CONTROLLING OFFICE NAME AND ADDRESS DEPARTMENT OF THE ARMY US Army Corps of Engineers Washington, DC 20314-1000	12. REPORT DATE November 1984	
	13. NUMBER OF PAGES 106	
14. MONITORING AGENCY NAME & ADDRESS (if different from Controlling Office) US Army Engineer Waterways Experiment Station Geotechnical Laboratory PO Box 631, Vicksburg, Mississippi 39180-0631	15. SECURITY CLASS. (of this report) Unclassified	
	15a. DECLASSIFICATION/DOWNGRADING SCHEDULE	
16. DISTRIBUTION STATEMENT (of this Report) Approved for public release; distribution unlimited.		
17. DISTRIBUTION STATEMENT (of the abstract entered in Block 20, if different from Report)		
18. SUPPLEMENTARY NOTES Available from the National Technical Information Service, 5285 Port Royal Road, Springfield, Virginia 22161		
19. KEY WORDS (Continue on reverse side if necessary and identify by block number) Swelling soils (LC) Foundations (LC) Structural engineering--Research (LC) Soil mechanics (LC)		
20. ABSTRACT (Continue on reverse side if necessary and identify by block number) The Medical Field Services School at Fort Sam Houston, San Antonio, Tex., was constructed in 1970 and 1971. The performance of the structure was monitor- ed using free-standing bench marks, grade-beam bench marks, and strain gages in three drilled piers. Performance of the structure was predicted using five analysis techniques presented in the literature. Actual and predicted perfor- mances were compared. Based on these results, the five analysis techniques are compared in their ability to predict the performance of a drilled pier foundation.		

DD FORM 1 JAN 73 1473

EDITION OF 1 NOV 65 IS OBSOLETE

Unclassified

SECURITY CLASSIFICATION OF THIS PAGE (When Data Entered)

PREFACE

This report was prepared by Mr. Mark Simmons, staff member of the Foundations and Materials Branch, U. S. Army Engineer Fort Worth District (FWD). The report was reviewed by Dr. James C. Armstrong, Dr. Judith Corely, Dr. Thomas Petry, and Dr. Max Spindler of the University of Texas at Arlington and Mr. William R. Stroman, FWD.

The report is a valuable contribution to the results of the Military RDT&E Project AT40, Task EO, Work Unit 006, "Methodology for Design of Drilled Piers in Cohesive Soils," and augments the methodology documented in Technical Report GL-84-5, "Methodology for Design and Construction of Drilled Shafts in Cohesive Soils," published by the U. S. Army Engineer Waterways Experiment Station (WES), Vicksburg, Miss. The report verifies and describes application of program HEAVE documented in Miscellaneous Paper GL-82-7, "User's Guide for Computer Program HEAVE," published by WES, through analysis of instrumented full-scale shaft foundations of a military structure. The report was reviewed by Dr. Lawrence D. Johnson, Soil Mechanics Division (SMD), Geotechnical Laboratory (GL), and the Office, Chief of Engineers (OCE), US Army, prior to publication by WES. Publication of this report was under the general supervision of Mr. Clifford L. McAnear, Chief, SMD, and Dr. William F. Marcuson III, Chief, GL.

The Commander and Director of WES was COL Tilford C. Creel, CE. The Technical Director was Mr. Fred R. Brown.



Accession For	
NTIS GRA&I	<input checked="" type="checkbox"/>
DTIC TAB	<input type="checkbox"/>
Unannounced	<input type="checkbox"/>
Justification	
By _____	
Distribution/	
Availability Codes	
Dist	Avail and/or Special
A-1	

## CONTENTS

	<u>Page</u>
PREFACE . . . . .	1
CONVERSION FACTORS, U. S. CUSTOMARY TO METRIC (SI) UNITS OF MEASUREMENT . . . . .	4
CHAPTER 1: INTRODUCTION . . . . .	5
CHAPTER 2: REVIEW OF LITERATURE . . . . .	6
2.1 Shrink/Swell Mechanisms . . . . .	6
2.2 Engineering Analyses . . . . .	8
2.2.1 General . . . . .	8
2.2.2 van der Merwe's Correlation . . . . .	10
2.2.3 Vijayvergia and Ghazzaly's Correlation . . . . .	14
2.2.4 McClelland and Sullivan's Method . . . . .	14
2.2.5 Corps of Engineers Method . . . . .	17
2.2.6 Computer Program HEAVE . . . . .	19
CHAPTER 3: RESEARCH PROGRAM . . . . .	25
3.1 General . . . . .	25
3.2 Medical Field Services School . . . . .	25
3.2.1 General . . . . .	25
3.2.2 Subsurface Conditions . . . . .	25
3.2.3 Foundation . . . . .	26
3.2.4 Instrumentation . . . . .	33
CHAPTER 4: PREDICTION OF HEAVE . . . . .	38
4.1 Analysis Assumptions . . . . .	38
4.1.1 Subsurface Profile . . . . .	38
4.1.2 Depth of the Active Zone . . . . .	39
4.1.3 Typical Pier . . . . .	39
4.1.4 Uplift on the Pier Shaft . . . . .	39
4.1.5 Final Pore Water Pressure Distribution . . . . .	42
4.2 van der Merwe's Correlation . . . . .	43
4.3 Vijayvergia and Ghazzaly's Correlation . . . . .	43
4.4 McClelland and Sullivan's Method . . . . .	45
4.5 Corps of Engineers Method . . . . .	46
4.6 Computer Program HEAVE . . . . .	47
4.6.1 Input Data . . . . .	47
4.6.2 Suction Model Results . . . . .	50
4.6.3 Mechanical Model Results . . . . .	52
4.6.4 Further Analyses . . . . .	53
CHAPTER 5: ANALYSIS OF INSTRUMENTATION . . . . .	59
5.1 Free Standing Benchmarks . . . . .	59
5.2 Grade Beam Benchmarks . . . . .	60
5.3 Strain Gages . . . . .	62
5.3.1 Initial Analyses . . . . .	65
5.3.2 Creep of Reinforced Concrete . . . . .	67
5.3.3 Reanalysis of Strain Gage Data . . . . .	71
5.4 Assessment of Building Performance . . . . .	80

	<u>Page</u>
CHAPTER 6: PREDICTED PERFORMANCE VERSUS ACTUAL PERFORMANCE . . . . .	82
6.1 General . . . . .	82
6.2 van der Merwe . . . . .	82
6.3 Vijayvergia and Ghazzaly . . . . .	84
6.4 McClelland and Sullivan . . . . .	85
6.5 Corps of Engineers . . . . .	85
6.6 Computer Program HEAVE . . . . .	86
6.6.1 Mechanical Model . . . . .	86
6.6.2 Suction Model . . . . .	87
6.6.3 Conclusions . . . . .	88
CHAPTER 7: CONCLUSIONS . . . . .	89
CHAPTER 8: RECOMMENDATIONS FOR FURTHER STUDY . . . . .	90
REFERENCES . . . . .	91
APPENDIX A: SWELL PRESSURE TEST RESULTS . . . . .	A1
APPENDIX B: CONSOLIDATION-EXPANSION TEST RESULTS . . . . .	B1
APPENDIX C: COMPUTATION OF UPLIFT FORCES ON DRILLED PIER SHAFT . . . . .	C1

CONVERSION FACTORS, U. S. CUSTOMARY TO METRIC (SI)  
UNITS OF MEASUREMENT

U. S. customary units of measurement used in this report can be converted to metric (SI) units as follows:

<u>Multiply</u>	<u>By</u>	<u>To Obtain</u>
feet	0.3048	metres
inches	2.54	centimetres
kips (force) per square foot	47.88026	kilopascals
kips (mass)	453.5924	kilograms
pounds (force) per square inch	6894.757	pascals
pounds (mass) per cubic foot	16.01846	kilograms per cubic metre
tons (force) per square foot	95.76052	kilopascals
tons (2000 pounds, mass)	907.1847	kilograms

PREDICTED AND ACTUAL PERFORMANCE OF A  
STRUCTURE IN EXPANSIVE SOILS

CHAPTER 1

INTRODUCTION

Recognition of expansive soils as a problem began to gain widespread attention in the 1950's and early 1960's with the publication of papers by researchers such as Jennings and Knight or van der Merwe, all of South Africa. From this early beginning much research has been performed and numerous papers, technical reports, and books have been published discussing expansive soil behavior and methods for predicting its behavior. This work and published data have done much to advance the understanding of expansive soils; however, there are still areas without clear answers, attesting to the difficulty and magnitude of the problems associated with expansive soils.

In 1973 it was estimated that 10 percent of the over 250,000 homes constructed on expansive soils would experience significant damage(8). Repairs to these damaged homes would cost as much as \$15,000 each(6). Current estimates place the annual damage due to expansive soils at \$2.3 billion in the United States alone, which is twice as much as all other natural disasters combined(9). It is estimated that by the year 2000 this loss will increase to \$4.5 billion per year (1978 dollars) unless application of improved design procedures are used to lessen the damage from expansive soils.

The first step in predicting expansive soil behavior and avoiding damage is to gain an understanding of the expansive soil phenomenon and why it occurs.

## CHAPTER 2

### REVIEW OF LITERATURE

2.1 Shrink/Swell Mechanisms. Cyclic shrinkage and swelling of expansive soils are due to the migration of water into and out of the soil structure. In a soil with a well developed structure, water loss first occurs in the cracks or voids between the soil pedes or crumbs. The volume of water lost is greater than the volume change of the soil and this is referred to as structural shrinkage. The next water loss occurs within the soil ped itself and the volume of water lost equals the volume change of the soil. No air enters the soil voids and water is pulled from the interior of the soil ped. This process is called normal shrinkage. Residual shrinkage occurs when air begins to enter the soil ped and the amount of water lost exceeds the volume change of the soil(18). Figure 2.1 shows a plot of soil volume versus water content to illustrate this concept.

The forces causing these volume changes are explained using a variety of concepts, one of which is soil suction. Soil suction is composed of two parts, matrix suction and osmotic suction. Matrix suction is "the negative gauge pressure relative to the external gas pressure on the soil water, to which a solution identical in composition with the soil water must be subjected in order to be in equilibrium through a porous membrane wall in the soil water(1). Matrix suction is pressure dependent and can be measured using a piezometer(11). Osmotic suction

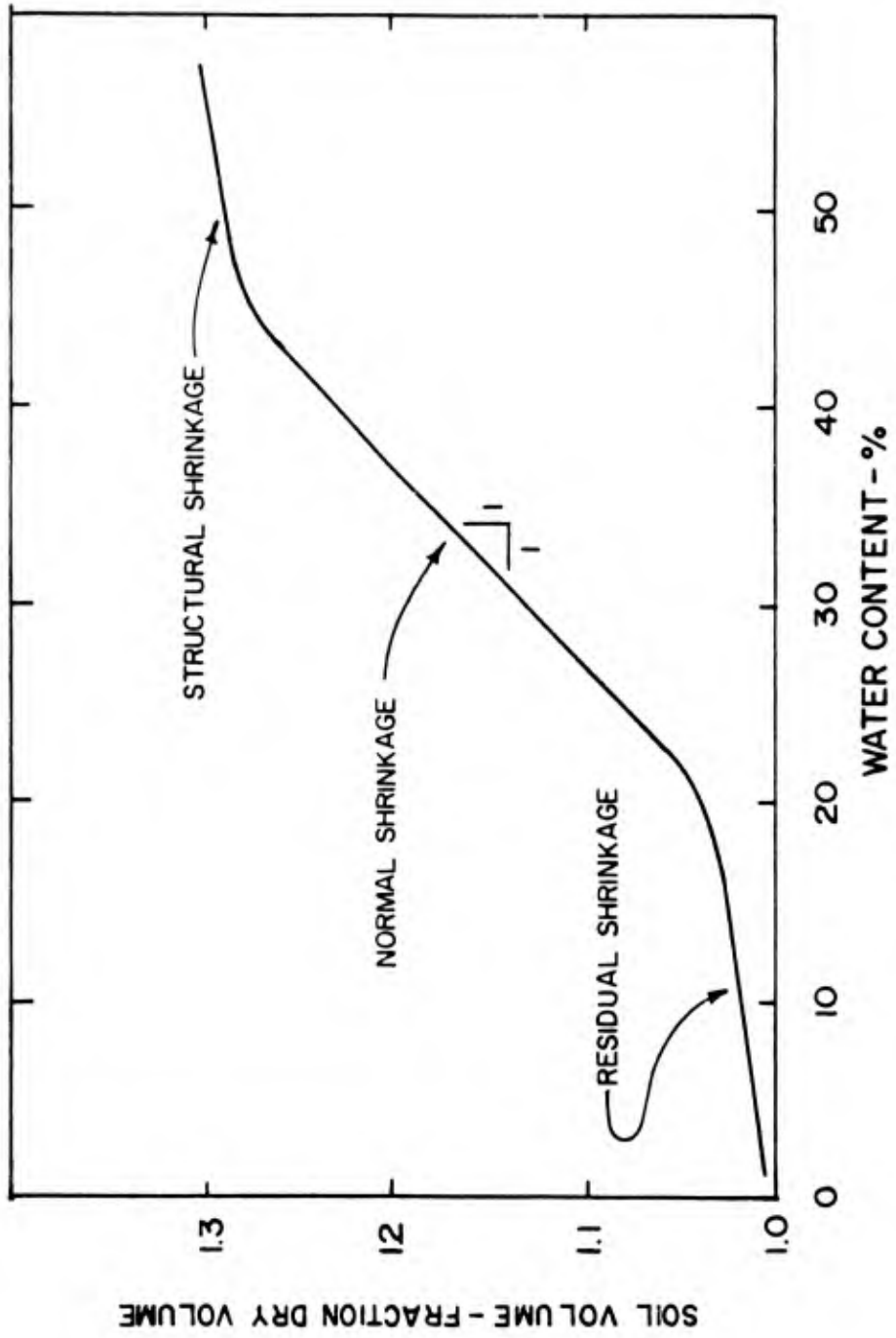


Figure 2.1 Soil volume versus water content

is "the negative guage pressure to which a pool of pure water must be subjected in order to be in equilibrium through a semipermeable membrane (i.e. permeable to water only) with a pool of water containing a solution identical in composition with the soil water(1)."

**2.2 Engineering Analyses.** A discussion of expansive soils behavior and methods for predicting this behavior will be discussed in the following paragraphs.

**2.2.1 General.** The behavior of expansive soils is very complex and is affected by a wide range of variables such as soil characteristics, initial moisture content, climate, vegetation, in situ density, slope of the site, and changes brought about by man's action. The variables can be divided into two categories, environmental and inherent properties. Many of these variables, such as climate, are qualitative and beyond the control of the engineer. Others, such as moisture content can be measured, and with varying degrees of success controlled. Analytical techniques concentrate on the measurable and predictable quantities, leaving the engineer to rely on judgement concerning the unmeasurable quantities. The analysis techniques for expansive soil behavior can be separated into two categories, empirical and analytical. The empirical analyses involve correlations between percent swell and/or swell pressure and some easily determined index property, such as liquid limit, plasticity index, or dry density. The Atterberg limits are the most commonly used index property and appear in almost every empirical equation either as the liquid limit or plasticity index.

The liquid and plastic limits represent the upper and lower bounds of plastic behavior while the plasticity index represents the range of water contents over which the soil acts as a plastic material(18). When an expansive soil is at its liquid limit most of the water is interlayer water that is immobilized by the clay particles(11). At this point the clay will be moisture satisfied and will not expand further. The plastic limit is at the other extreme. The soil has reduced in volume to the point where only interparticle repulsion forces are preventing any further volume reductions and it is in a very moisture deficient condition. This can be related to the normal shrinkage of a soil ped where the majority of the volume change occurs. The range of water contents over which normal shrinkage occurs corresponds to the plasticity index with the liquid limit near the break point between normal and structural shrinkage and the plastic limit near the break point between normal and residual shrinkage. The compatibility of Atterberg limits with the concept of normal shrinkage is one reason why Atterberg limits are used in the empirical correlations. Another factor is the well documented evidence which shows that the more expansive clay minerals have higher liquid limits and plasticity indices(17). They are also inexpensive and easily performed tests which further enhances their attraction as correlation factors.

The analytical techniques assume heave and settlement are similar phenomenon that can be described with similar equations. Three types of consolidometer tests are commonly used; and recently soil suction tests results have begun to come into use.

The consolidometer tests are called the free swell, swell pressure and expansion-consolidation tests. All of the tests are similar in that a sample is placed in an oedometer and confined at some predetermined pressure, normally overburden pressure. At this point the test procedures differ and will be discussed separately in the following paragraphs.

In the free swell test, after the initial void ratio is noted, the sample is unloaded to a nominal seating load, normally 0.1 TSF,\* and allowed free access to water. The sample is allowed to swell completely. When swelling stops, a standard consolidation test is then conducted. The percent swell is the change in void ratio, at the overburden pressure, divided by the total initial volume of the sample.

Two empirical correlations along with use of the swell pressure, expansion-consolidation and soil suction tests in prediction of expansive soils behavior will be covered in greater detail in the next portion of this thesis and a presentation on the analyses of the data will be presented following that.

2.2.2 van der Merwe's Correlation(10). D.H. van der Merwe (1964) described a method to predict heave beneath a building. Although it was not expressly stated, this technique was probably intended for use with slab-on-grade foundations. However, it can be used to predict heave at any depth. This technique is quite simple to use and the testing required is inexpensive and standard in typical foundation analyses.

---

\* A table of factors for converting U. S. customary units of measurement to metric (SI) units is presented on page 4.

A potential expansiveness at the ground surface of 0, 1/4, 1/2, or 1 inch/foot of depth is assigned to each soil stratum, using the results of Atterberg limit and gradation testing, and the chart shown on Figure 2.2. The potential expansiveness is multiplied by a factor  $F_D$  which takes into account the effects of increase in overburden pressure with depth, decreasing change in moisture content with depth, etc.  $F_D$  is computed using

$$D = k (\log F_D) \quad \text{Eqn 2.1}$$

$D$  = depth below the ground surface (negative number)

$k$  = constant = 20

$F_D$  = factor relating heave with depth

The value of  $k=20$  was selected after comparing measured values of heave at several sites with computed values of heave using a variety of  $k$  values. See Figure 2.3 for plot of  $F_D$  with  $k=20$ .

The total heave is equal to the summation of the potential heave multiplied by  $F_D$ .

$$\text{Total Heave} = \sum^n F_D \times (PE)_D \quad \text{Eqn 2.2}$$

$F_D$  = factor relation heave with depth at depth  $D$

$(PE)_D$  = potential expansiveness in inches/foot at depth  $D$

$n$  = depth of active zone in feet

The disadvantages of this technique are that it was developed for South African soils; thus the  $k=20$  may not be correct for other areas

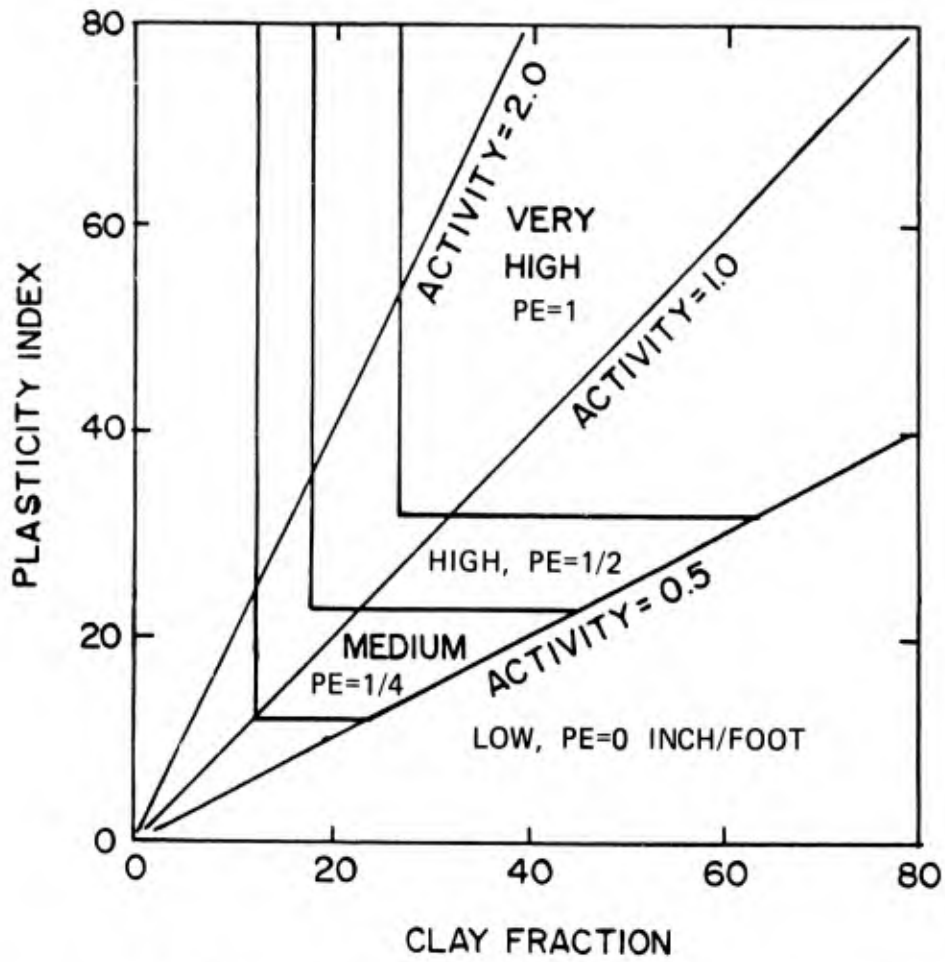


Figure 2.2 Determination of potential expansiveness, PE

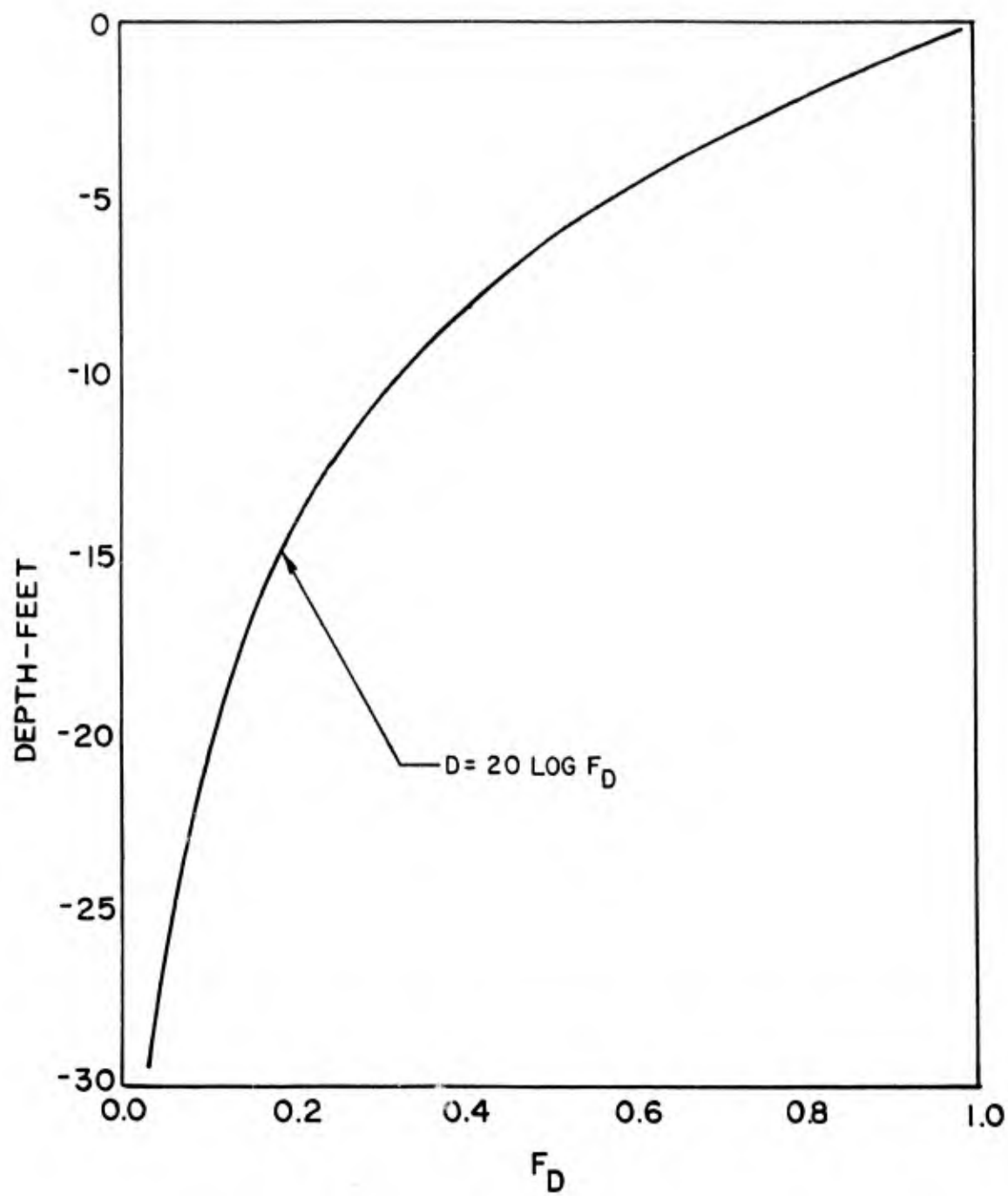


Figure 2.3 Depth correction factor

and the technique is for slabs on grade not drilled piers. Its advantages are that testing is minimal and inexpensive; only a set of Atterberg limits and a hydrometer test are needed; and its simplicity in application.

2.2.3 Vijayvergia and Ghazzaly's Correlation(16). Vijayvergia and Ghazzaly used the results of approximately 270 swell tests having a "wide geographic coverage" to perform a series of regression analyses to relate percent swell and swell pressure with other soil properties such as Atterberg limits, dry density and moisture content. The test specimens were obtained primarily from Texas with a few from Oklahoma, California, Arkansas, Israel and India.

Four relationships developed as follows:

$$\text{Log } S = 1/12 (0.4 \text{ LL} - W + 5.5) \quad \text{Eqn 2.3}$$

$$\text{Log } S = 1/19.5 (\gamma_d + 0.65 \text{ LL} - 139.5) \quad \text{Eqn 2.4}$$

$$\text{Log } P = 1/12 (0.4 \text{ LL} - W - 0.4) \quad \text{Eqn 2.5}$$

$$\text{Log } P = 1/19.5 (\gamma_d + 0.65 \text{ LL} - 139.5) \quad \text{Eqn 2.6}$$

S = % Swell

P = Swell Pressure in TSF

LL = Liquid Limit in %

W = Water Content in %

$\gamma_d$  = Dry Density in pcf

The coefficients of correlation were 0.7 or better.

2.2.4 McClelland and Sullivan's Method(13). This method utilizes a

swell pressure test which first involves placing a sample in an oedometer and confining it at overburden pressure. The sample is then allowed free access to water while the tendency to swell is controlled by placing additional load on the sample to maintain a constant volume. When swelling stops the sample is allowed to rebound back to a nominal load, normally 0.1 TSF.

The first step in analysis of the results is to determine the initial and final effective vertical stresses. The following equations are used to compute these values.

$$\sigma_i'' = P_o + X p_i'' \quad \text{Eqn 2.7}$$

$$\sigma_f'' = P_o + \Delta P + p_f'' \quad \text{Eqn 2.8}$$

$\sigma_i''$  = initial effective vertical stress

$\sigma_f''$  = final effective vertical stress

$P_o$  = overburden pressure

$\Delta P$  = increase in pressure due to the structure

$X$  = factor relating portion of soil suction that contributes to effective stress, after Blight see Figure 2.4(3)

$p_i''$  = initial pore water pressure =  $P_{exp} - P_o$

$p_f''$  = assumed final pore water pressure

$P_{exp}$  = expansion pressure

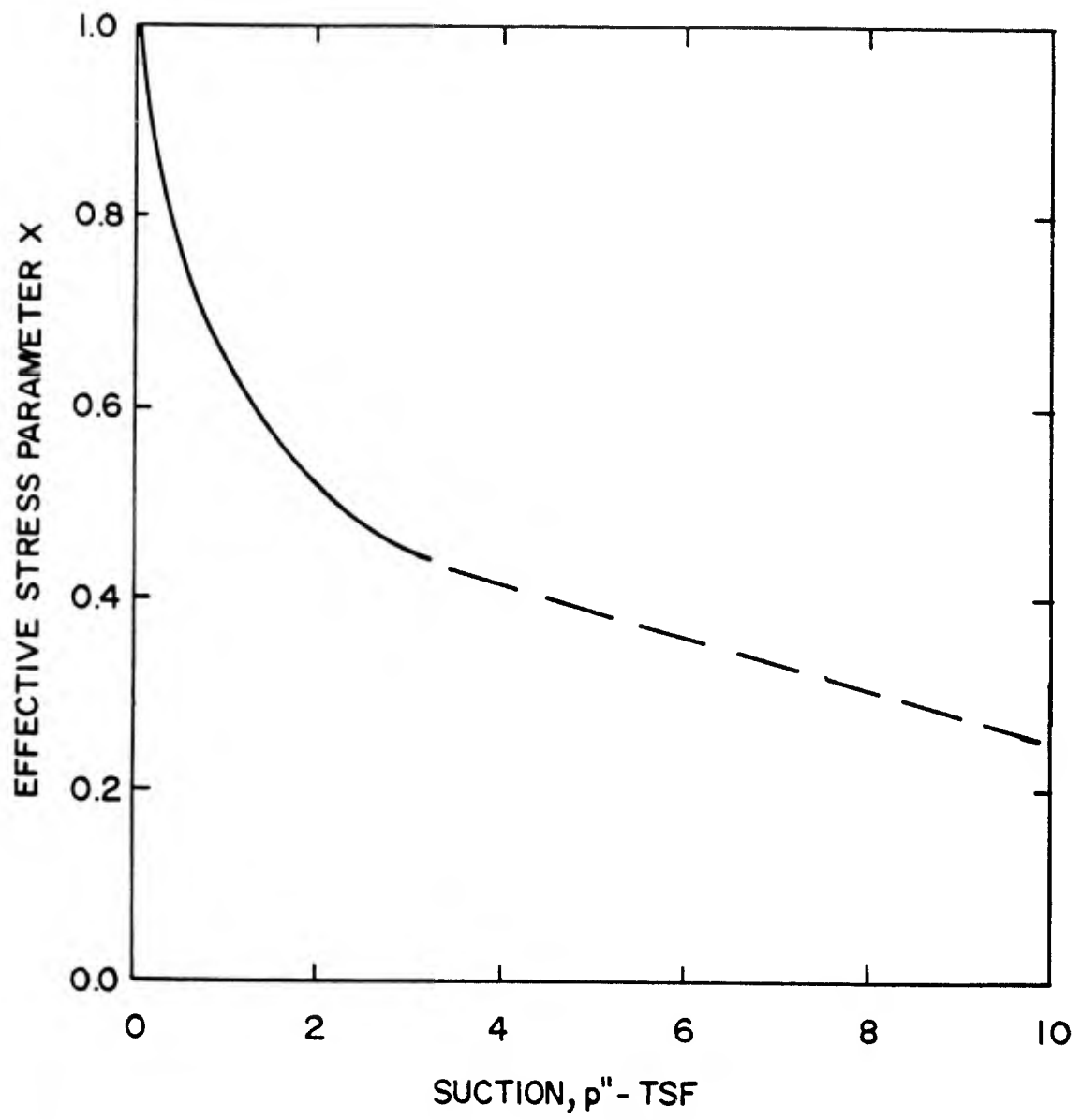


Figure 2.4 Effective stress parameter X versus suction

Once the initial and final effective vertical stresses are known, their corresponding void ratios can be selected from the rebound portion of the void ratio versus pressure plot. Heave is then computed as follows:

$$\frac{\Delta H}{H} = \frac{e_f - e_i}{1 + e_0} \quad \text{Eqn 2.9}$$

$\Delta H$  = heave

$e_f$  = void ratio corresponding to  $\sigma_f''$

$e_i$  = void ratio corresponding to  $\sigma_i''$

$e_0$  = initial void ratio

$H$  = thickness of stratum under consideration

A typical void ratio - log pressure plot for the swell pressure test is shown on Figure 2.5.

2.2.5 Corps of Engineers Method (5). This technique is used by the Fort Worth District to predict heave. The first step is to conduct a consolidation-expansion test.

The test involves placing a sample in an oedometer and loading it to overburden pressure. The sample is then allowed free access to water while controlling the tendency to swell by adding additional load, thus maintaining a constant volume. When the tendency to swell stops, a con-

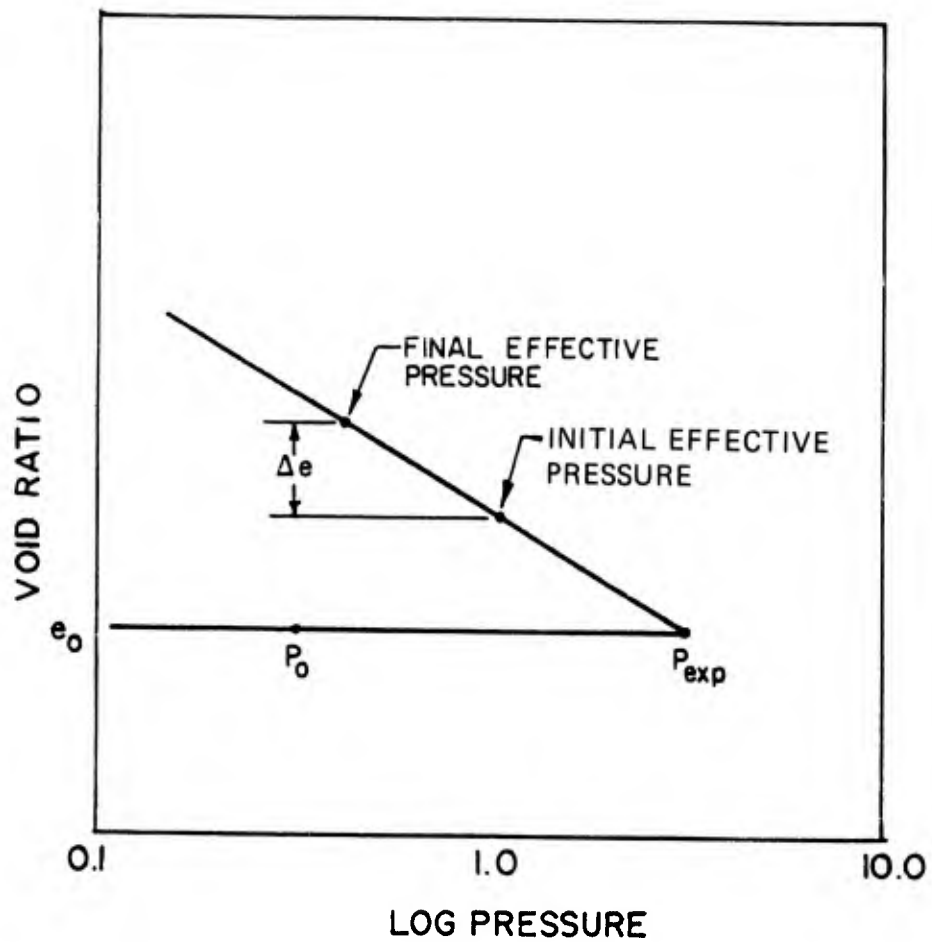


Figure 2.5 Swell pressure test

solidation test is conducted and then the sample is allowed to rebound back to a nominal load of 0.1 TSF.

The first step in the analysis is to construct a line parallel to the steepest portion of the rebound curve through the point where expansion stopped. Next overburden pressures ( $P_0$ ) and overburden plus additional structural pressure ( $P_0 + P$ ) are computed and their corresponding void ratio's are determined using the void ratio versus pressure plot. A typical example of the void ratio-pressure plot showing how the void ratios are selected is shown on Figure 2.6.

2.2.6 Computer Program HEAVE(5). A computer program to predict heave beneath a structure was developed by the U.S. Army Corps of Engineers at the Waterways Experiment Station in Vicksburg, Mississippi.

The program will solve for heave at the center and edge of a rectangular or strip foundation and at the center of a circular deep shaft using a mechanical model and a suction model.

The mechanical model requires data from consolidation-expansion tests and solves for heave in much the same manner as outlined in the previous section.

The suction model requires data from soil suction tests. This data is obtained using either the filter paper method or the thermocouple psychrometer method which will determine the total suction of the sample. Normally the thermocouple psychrometer method is used because it is easier to perform and requires less time.

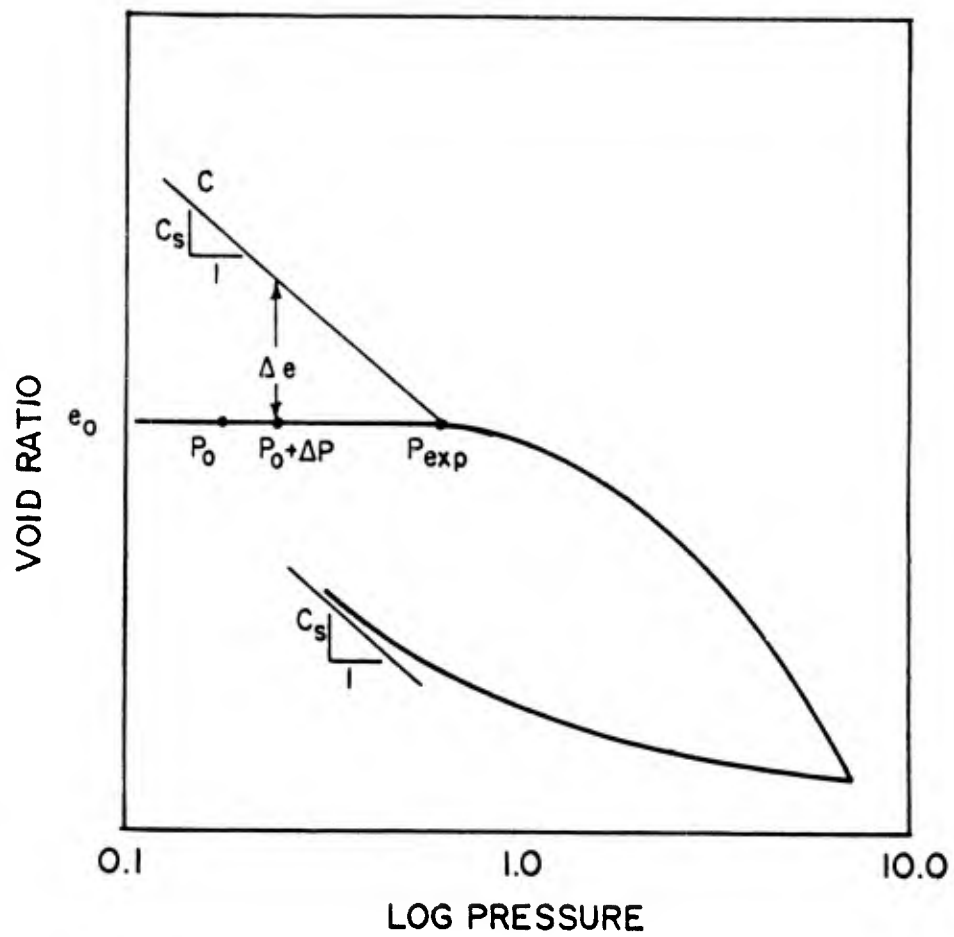


Figure 2.6 Consolidation-expansion test

Once the total suction is determined, it is plotted versus water content. Only the matrix suction is input into the program so if an osmotic suction component is present, it must be subtracted from the total suction. If the total suction versus water content is linear as in Figure 2.7a then there is no osmotic suction component and total suction equals matrix suction. If, however, the plot resembles Figure 2.7b, then the osmotic suction, which is that portion of the suction that ranges from the water content axis to the horizontal section of the curve, must be subtracted from the total suction to obtain the matrix suction.

Only matrix suction is used because at three test sections monitored by WES osmotic suction had no effect on results and unless the salt concentration in the pore fluid is altered, no effect would be expected.

The initial matrix suction is determined from the suction testing and is described by:

$$\tau_{mo}^0 = A + Bw \quad \text{Eqn 2.10}$$

$$\tau_{mo}^0 = \text{initial matrix suction}$$

A = suction intercept of soil suction plot

B = slope of soil suction plot

w = water content

The final matrix suction is determined using the following equation

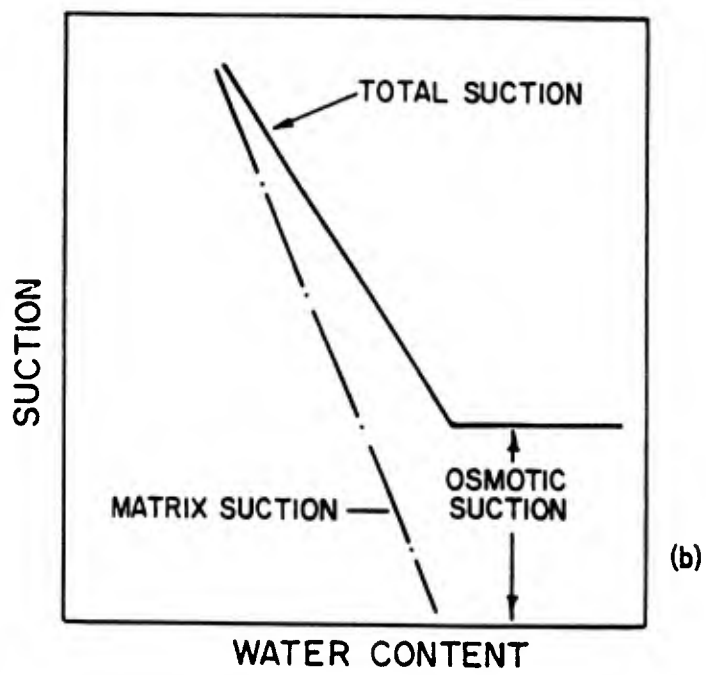
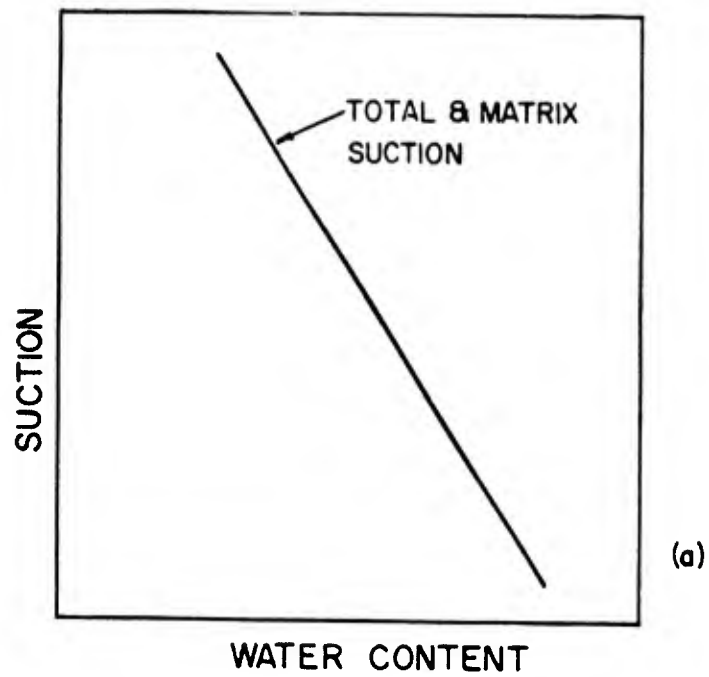


Figure 2.7 Determination of matrix suction

$$\tau_{mf}^0 = \left( \frac{1+2K}{3} \right) \sigma_v'$$

Eqn 2.11

$\tau_{mf}^0$  = final matrix suction

K = coefficient of effective lateral earth pressure

$\sigma_v'$  = effective vertical earth pressure =  $\sigma_v - u_w$

$\sigma_v$  = final total vertical earth pressure

$u_w$  = final pore water pressure

Once the initial and final matrix suction are known, heave computations can be performed using the following equation:

$$\frac{\Delta H}{H} = \frac{e_f - e_i}{1+e_o} = \frac{C_T}{1+e_o} \log \frac{\tau_{mo}^0}{\tau_{mf}^0}$$

Eqn 2.12

$\Delta H$  = Heave

H = Stratum Thickness

$e_f$  = Final Void Ratio

$e_i$  = Initial Void Ratio

$e_o$  = In Situ Void Ratio

$C_T$  = Suction Index =  $\frac{\alpha G_s}{100 B}$

$\tau_{mo}^0$  = Initial Matrix Suction w/o Surcharge Pressure

$\tau_{mf}^0$  = Final Matrix Suction w/o Surcharge Pressure

$\alpha$  = Compressibility Factor, Approximately 1 for Saturated or Highly  
Plastic Clay

$G_s$  = Specific Gravity

$B$  = Slope of Soil Suction Curve

## CHAPTER 3

### RESEARCH PROGRAM

3.1 General. Five methods of predicting expansive soils behavior have been presented. These techniques will be used to predict the behavior of the Medical Field Services School (MFSS) located at Fort Sam Houston in San Antonio, Texas. The predictions will be compared with each other and with actual measurements taken from instrumentation installed during construction of the MFSS.

3.2 Medical Field Services School. A description of the MFSS along with information on the subsurface conditions and instrumentation installed to monitor its performance are contained in the following paragraphs.

3.2.1 General. Construction of the MFSS occurred during 1970 and 1971. The building serves as a school to train Army personnel as field corpsmen and contains classroom and administrative areas as well as a surgical amphitheater. It is a 3-story structure with a basement supported over a four foot crawl space. The exterior walls are precast, exposed aggregate, reinforced concrete panels and the interior walls are either concrete masonry blocks or sheet rock.

3.2.2 Subsurface Conditions. Nine borings were drilled prior to construction to delineate subsurface conditions and obtain samples for laboratory testing. The overburden materials encountered were 15 to 22 feet thick and consisted of alternating, discontinuous layers of high and

low plasticity clays (CL, CH) and clayey, cherty gravel (GC). The primary formation consisted of a clay shale tentatively identified as the Taylor formation, which is of Cretaceous age. It is a highly to slightly jointed sandy clay shale that becomes noticeably less jointed and more sandy at a depth of approximately 40 feet below natural grade. Weathering extended to a depth of approximately 58 feet. Below the weathered zone the shale is well cemented and not jointed. A plan view of the MFSS showing boring and subsurface profile locations is shown in Figure 3.1. Subsurface profiles A-A and B-B are shown on Figures 3.2 and 3.3, respectively.

The samples recovered from the borings were subjected to identification, moisture content, gradation, dry density, shear strength and expansion tests. Laboratory test results necessary for the analysis techniques used in this paper are shown graphically on Figures 3.4 through 3.6 and in Appendices A and B. Figure 3.4 is a plot of Atterberg limits and in situ moisture content with respect to depth. Figure 3.5 shows moisture content and dry density with respect to depth. Figure 3.6 shows the minus 2 micron, clay size fraction, and plasticity index with respect to depth. Swell pressure test results and expansion-consolidation test results are contained in Appendices A and B respectively.

**3.2.3 Foundation.** The foundation consists of drilled and underreamed, reinforced concrete piers bottomed at elevation 728 MSL, 41 to 46 feet

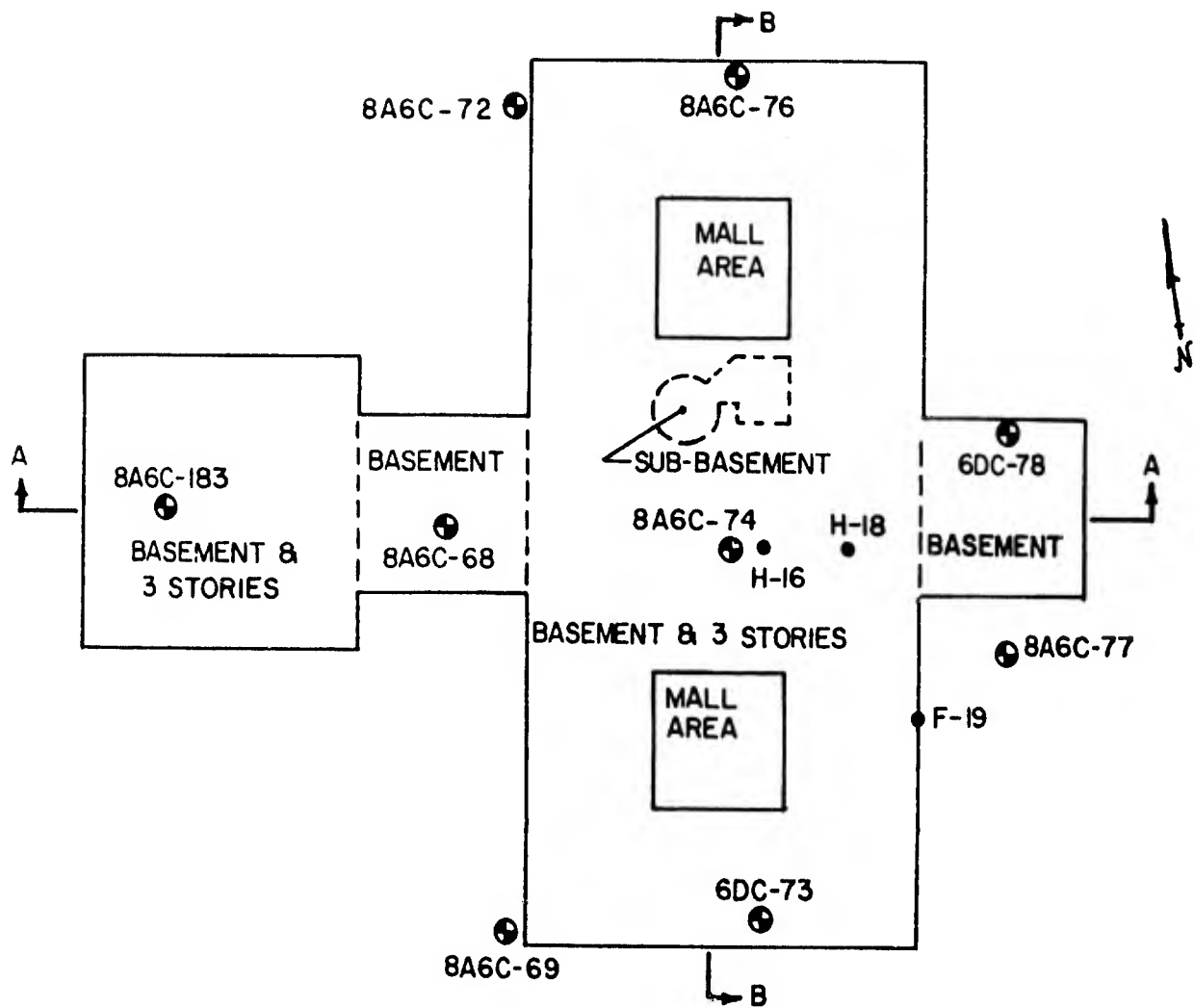


Figure 3.1 Planview of Medical Field Services school

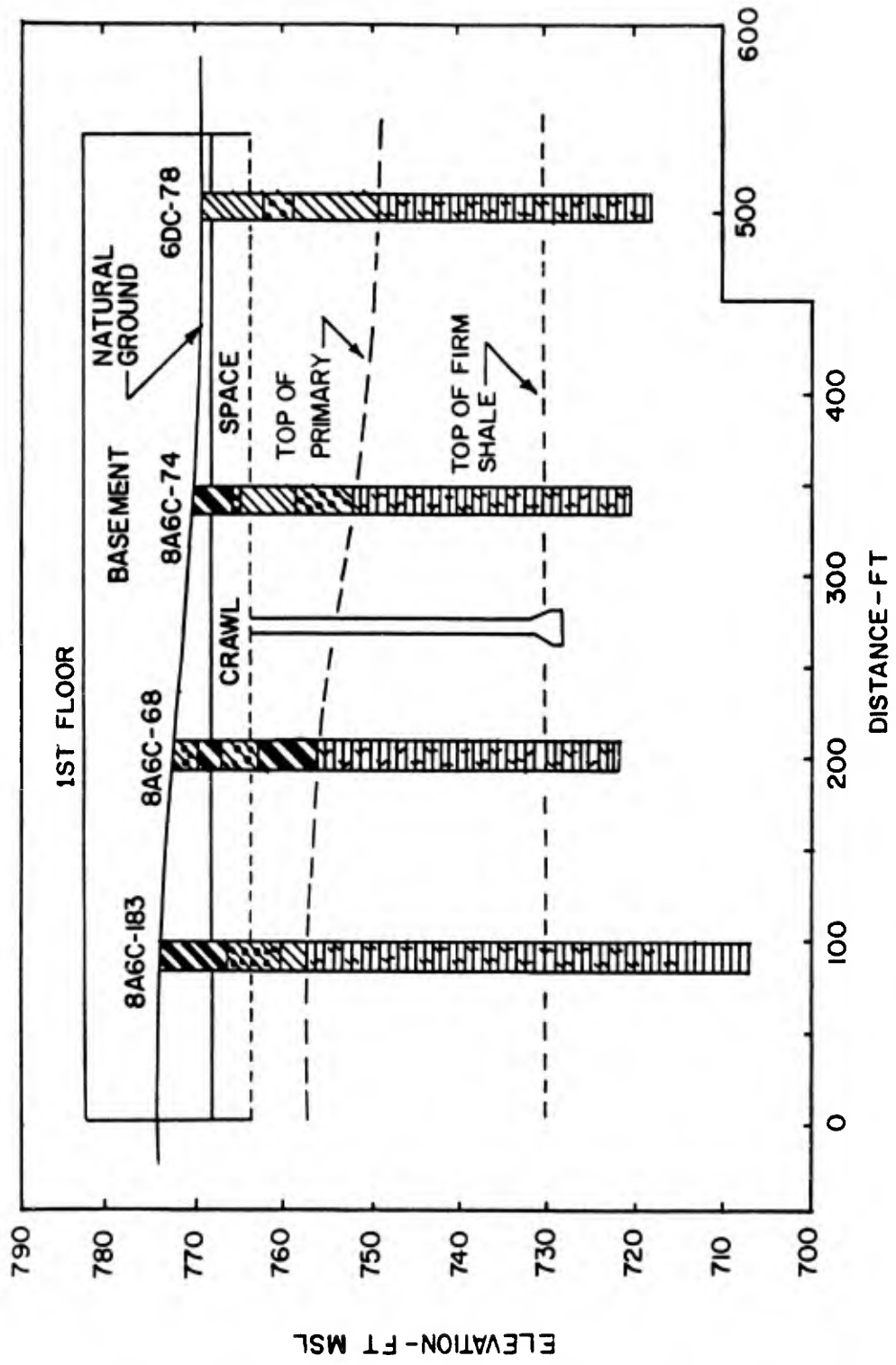


Figure 3.2 Section A-A

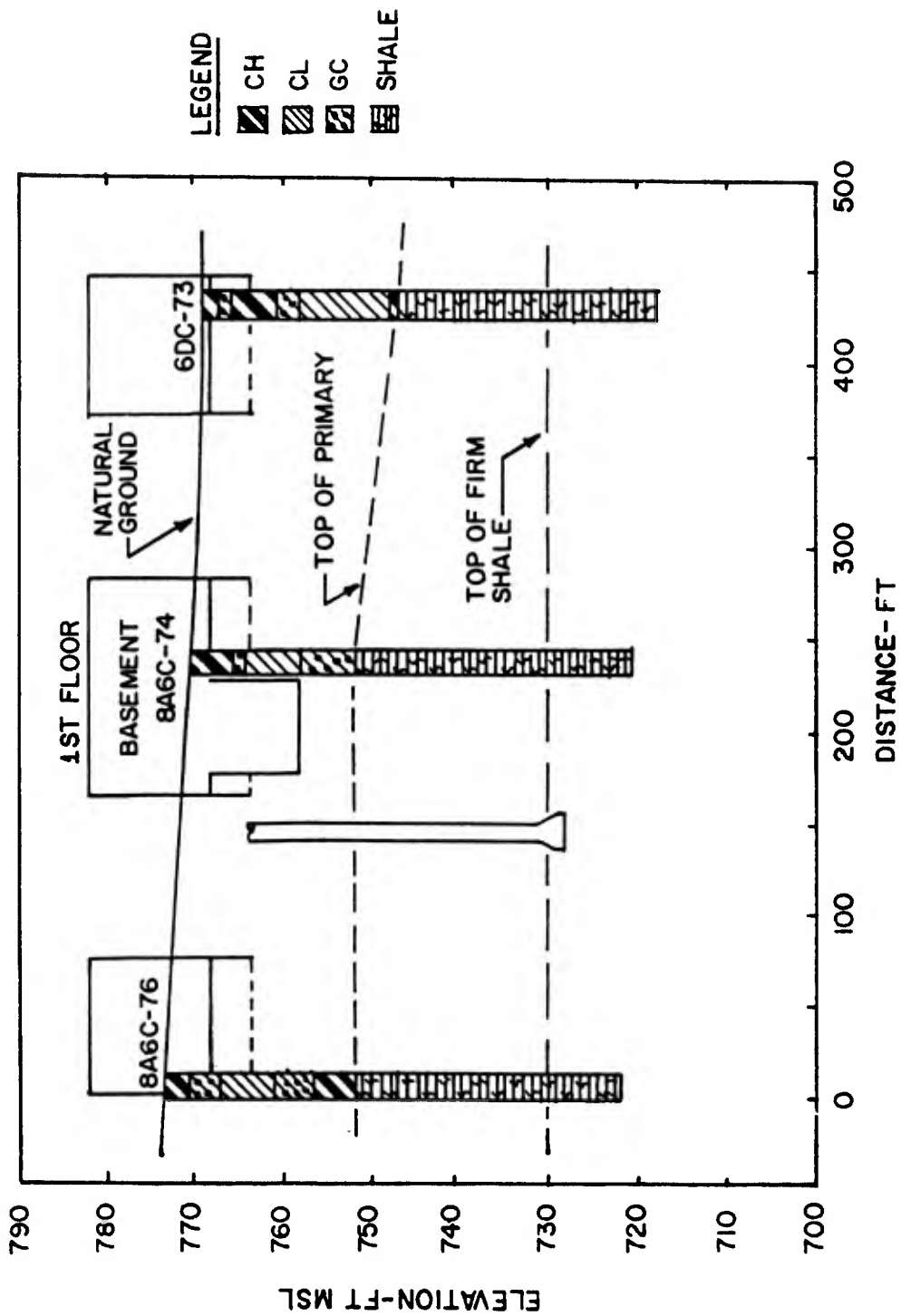


Figure 3.3 Section B-B

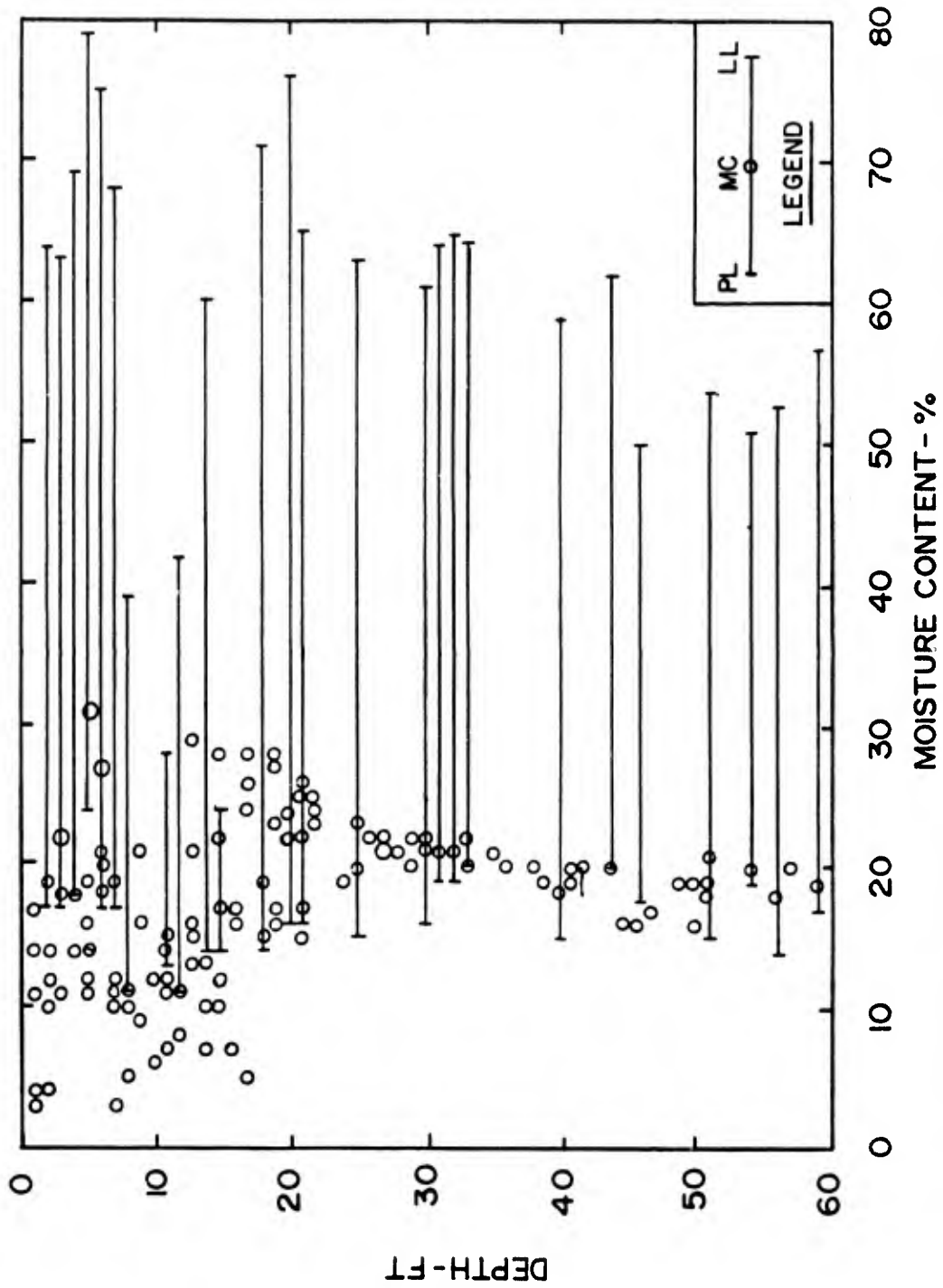


Figure 3.4 Moisture content and Atterberg limits versus depth

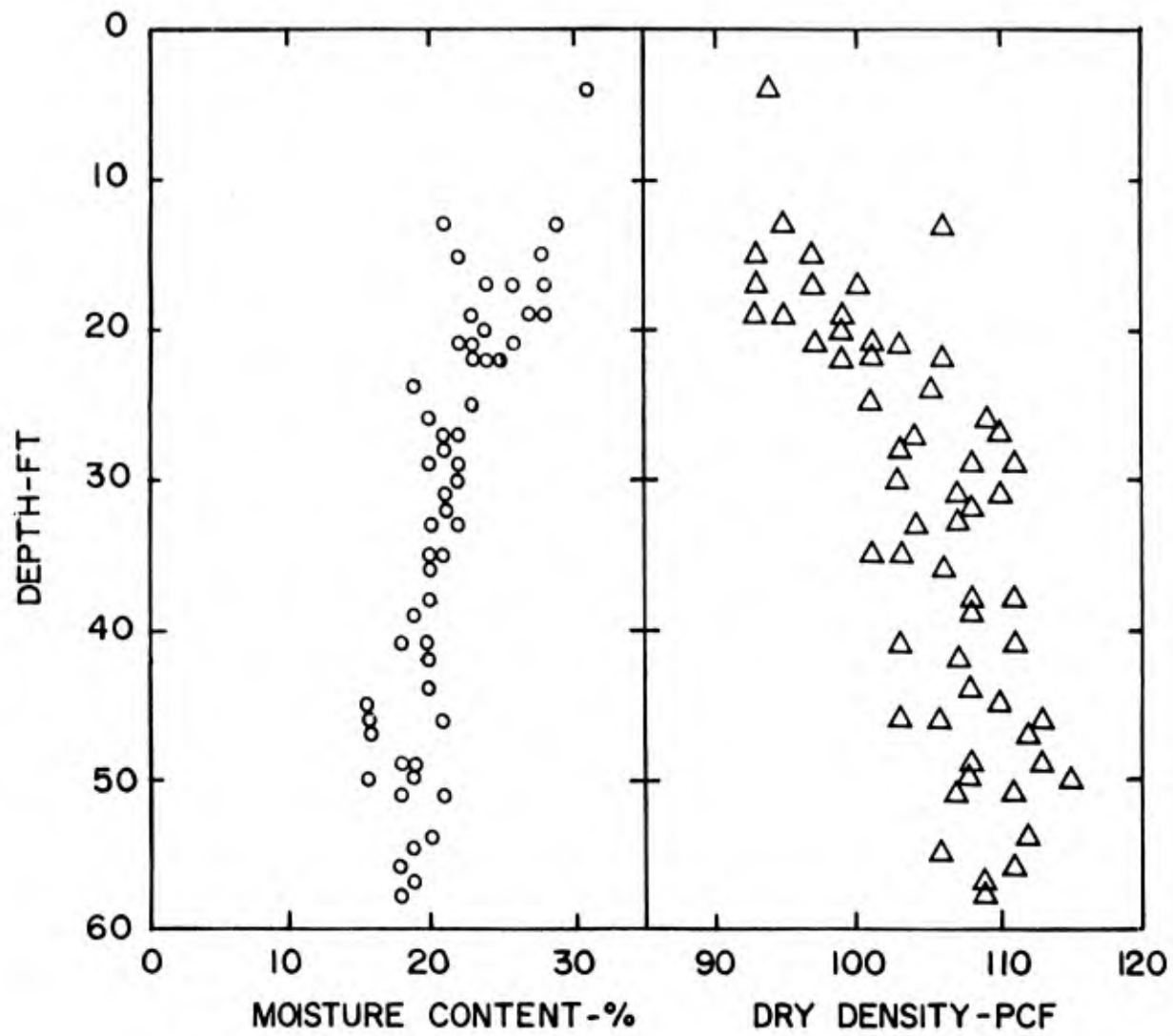


Figure 3.5 Moisture content and dry density versus depth

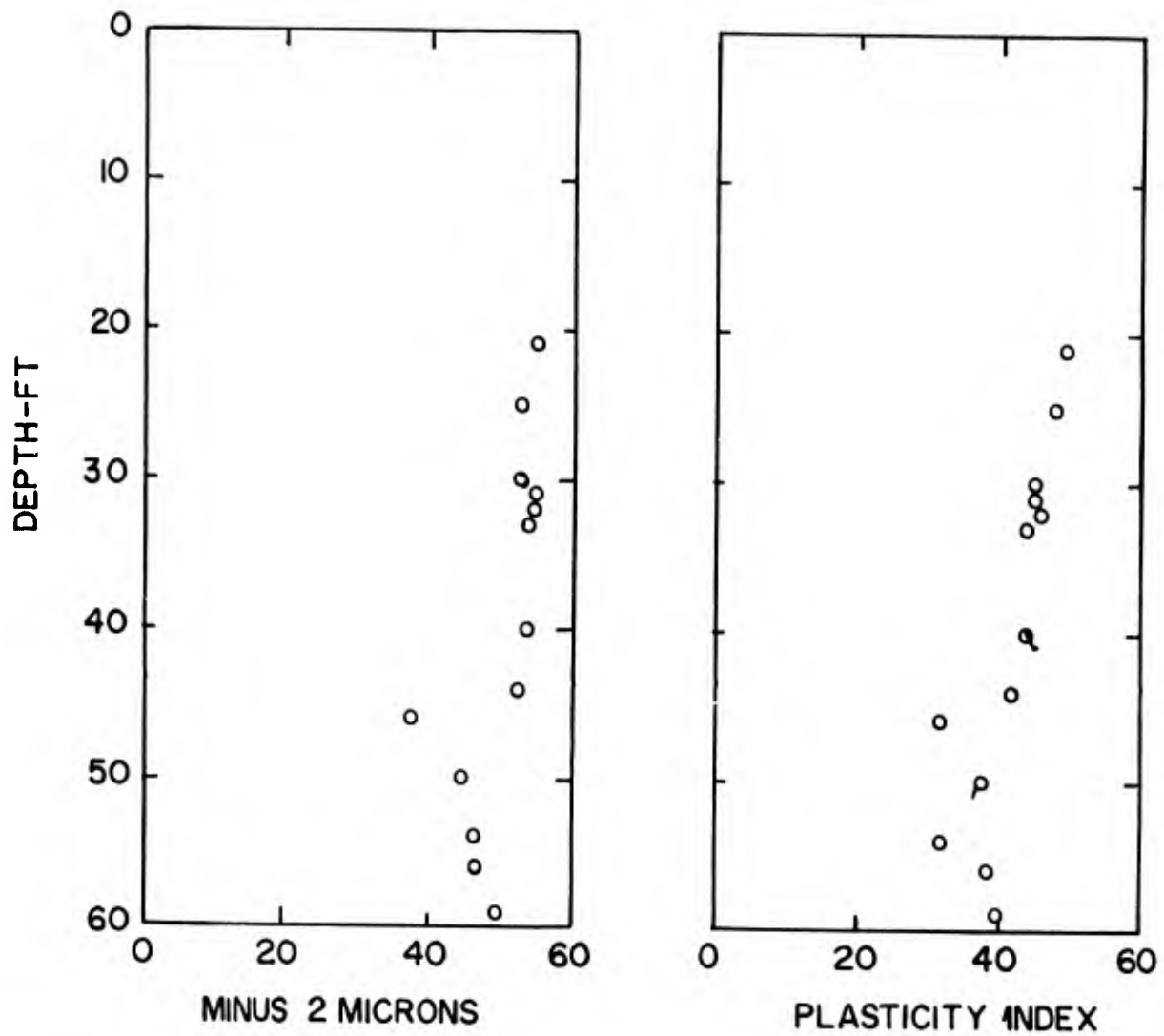


Figure 3.6 Minus 2 microns and plasticity index versus depth

below natural grade. The underreamed portions of the piers were sized using an allowable bearing capacity of 25.0 KSF. The load used to size the piers was the dead load plus 50% of the live load. A minimum of 2% vertical reinforcing steel was placed in each pier shaft and the shafts were spaced at least 10 feet apart to minimize angular distortions. Structural loads were transferred to the piers by a grade beam supported over a minimum 6-inch void. The basement floor is supported over a crawl space.

3.2.4 Instrumentation. Three types of instrumentation were installed to monitor movements. They included free standing bench marks, perimeter target bench marks built into the grade beams and strain gages on the reinforcing steel in three of the pier shafts.

Four free standing bench marks were set at various depths. BM-1 was set 2 feet below grade in clay, BM-2 was set 12.3 feet below grade in gravel, BM-3 was set 19.0 feet below grade which is 3.8 feet into the primary formation, and BM-4 was set 45.0 feet below grade which is 32.0 feet into the primary formation. Installation was accomplished by augering a 3-1/2 inch hole to the specified depth and driving a 3/8-inch rod with a cone on the end into the bottom of the hole. A 2-inch diameter, protective pipe was placed around the rod. Grease was pumped into the pipe until it flowed out the bottom of the pipe and back to the ground surface. A concrete guard was then placed around the bench mark. BM-4 was used as the datum to establish the initial elevation of all

bench marks on the project and as the reference for all subsequent surveys. See Figure 3.7 for a detail of this installation.

Thirty-seven perimeter target bench marks were installed in the grade beam. The bench mark consists of a 1/2-inch diameter by 3-inch brass bolt which was set in place and concrete for the grade beam poured around it. Approximately 1/2-inch of the bolt extends beyond the face of the grade beam. Initial elevations were determined to the nearest 0.01 foot. See Figure 3.8 for a detail of this installation.

Three of the piers were instrumented with strain gages as shown on Figure 3.9. Five strain gages at 6.5 to 7.0-centers were placed on a #11 A615 Grade 60 reinforcing bar beginning 3 feet from the top of the pier and ending 2 feet above the top of the underream. The first reading of the strain gages was made with the reinforcing bar resting horizontally so that an initial, nonstressed, reading could be taken as a datum. The bar was then placed in the center of the reinforcing cage and the concrete was placed around it.

The instrumentation was monitored frequently from 1970 through 1973 when readings were stopped. Another set of readings was made in the spring of 1982.

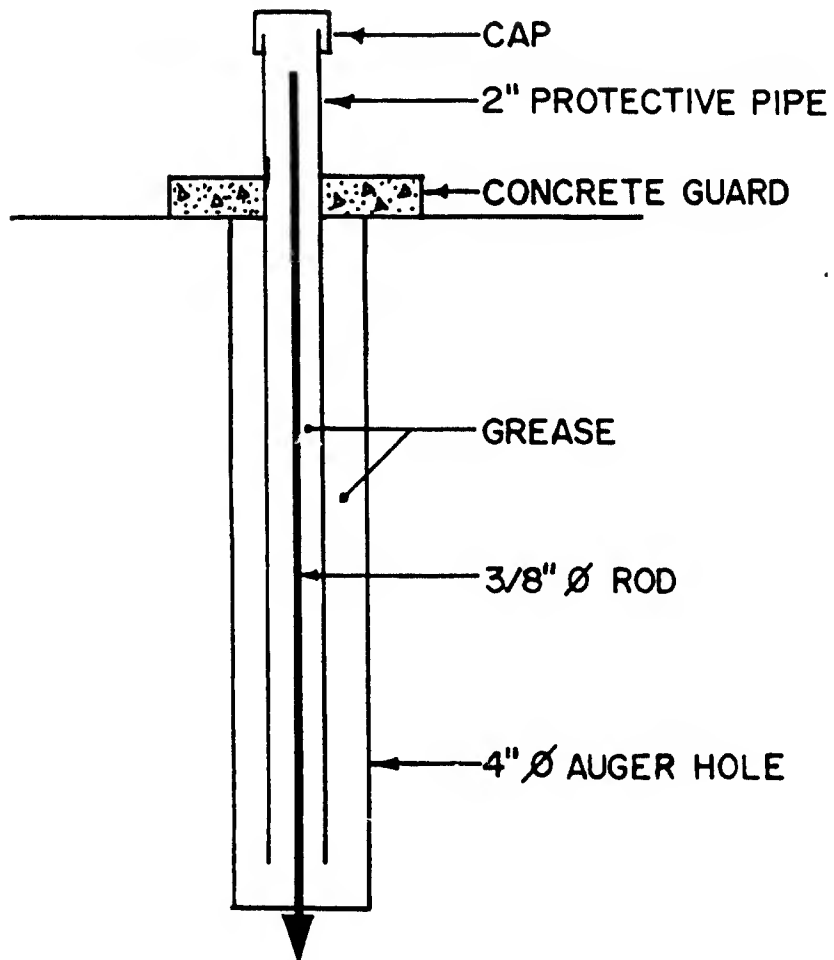


Figure 3.7 Free standing bench mark detail

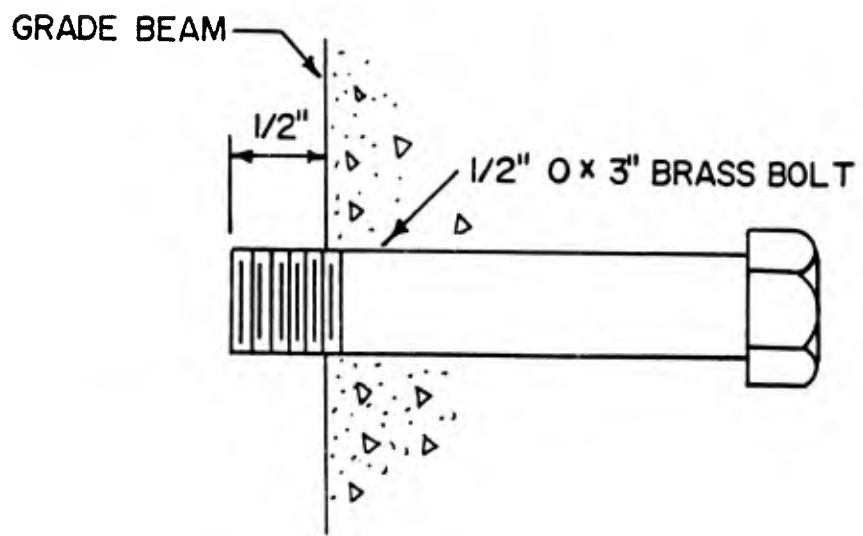
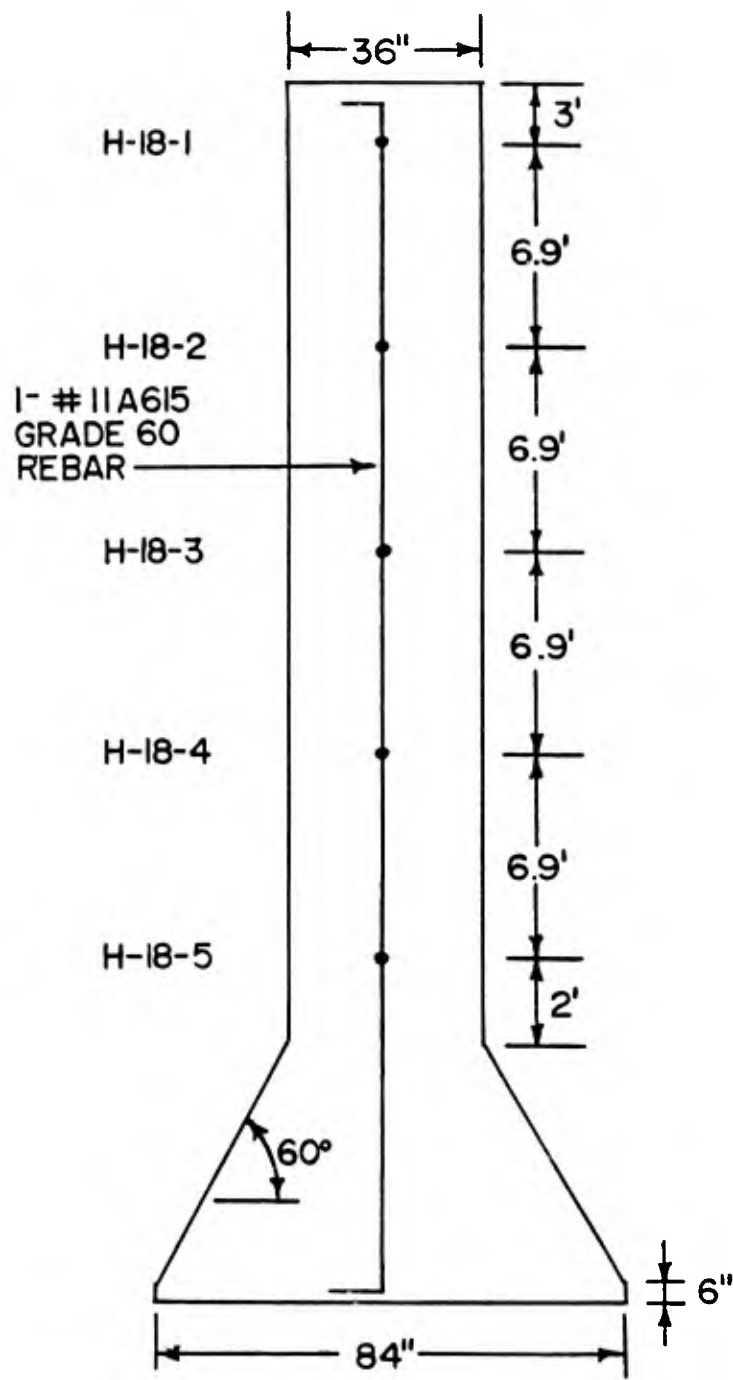


Figure 3.8 Grade beam bench mark detail



PIER H-18 (TYPICAL)  
N.T.S.

Figure 3.9 Strain gage installation detail

## CHAPTER 4

### PREDICTION OF HEAVE

4.1 Analysis Assumptions. A number of assumptions must be made when dealing with a project the size of the MFSS or a problem as complex as expansive soils to simplify analysis and design. Consequently a number of assumptions were made in preparation of this thesis to simplify computations and to define the upper and lower limits of heave using the best and worst possible conditions that might occur. The assumptions will be discussed individually in the following paragraphs.

4.1.1 Subsurface Profile. Subsurface conditions were discussed in Chapter 3. Attempts to correlate the clay and gravel strata between borings proved unsuccessful, therefore it was decided to assume the overburden consisted entirely of high plasticity clay. Since any low plasticity clay would be less expansive and any gravel would be nonexpansive, this is a conservative assumption but not an unreasonable one since a profile completely composed of expansive clay could occur at some point under the MFSS.

The overburden was assumed to extend to a depth of 20 feet where primary clay shale was encountered. The clay shale was assumed to be sandy and highly to slightly jointed to a depth of 40 feet where it became noticeably more sandy and less jointed. The drilled piers were assumed to bottom at a depth of 40 feet.

4.1.2 Depth of the Active Zone. The active zone was assumed to extend 20 feet below the bottom of the pier. This depth was selected after inspection of Figure 3.4, Atterberg limits and moisture content versus depth. At a depth of 40 feet (20 feet below the top of clay shale primary material) the moisture content values become relatively constant. Since this is a moisture content profile that has developed over a long period of time, it is reasonable to assume it is in equilibrium. It is assumed that piers bottomed in the clay shale allow water to infiltrate down the pier-soil interface and thus a source of free water will become available at the pier-soil interface similar to the free water source available at the overburden-primary interface prior to construction of the piers. Given sufficient time, a moisture content profile similar to the one from 20 to 40 feet will develop below the pier and volume changes due to moisture content variation will occur in this zone.

4.1.3 Typical Pier. Three piers with shaft/bell diameters of 30/72, 30/84 and 36/90 inches were instrumented. Plots of pressure versus depth for the three piers provide data so similar that they are interchangeable. Since the 30/84 is the intermediate size pier, it was selected for use in the computations and it is believed that extrapolation of the data for it to the other piers will result in negligible error.

4.1.4 Uplift on the Pier Shaft. The underreamed portion of the drilled piers were sized for an allowable bearing capacity of 25 KSF in end

bearing; however, it is recognized that some of the load will be taken out in skin friction reducing the total load applied at pier base. As water migrates down the pier-soil interface the adjacent soils will expand creating uplift on the pier shaft and even further reducing the load at the base on the pier. To determine the amount of load taken by the swelling soils adjacent to the pier shaft the following equation(7) was used:

$$S_T = \sum_0^Z [\gamma Z \tan^2 (45 + \phi/2) + 2c \tan (45 + \phi/2)] \tan \phi \cdot \Delta A \quad \text{Eqn 4.1}$$

$\gamma$  = Unit Weight

$Z$  = Depth

$\phi$  = Friction Angle from Drained Direct Shear Test

$C$  = Cohesion from Drained Direct Shear Test

$\Delta A$  = Surface Area of the Shaft

Values of  $C$  and  $\phi$  for the clay shale were determined using direct shear tests conducted on samples recovered during the subsurface investigations. Values of " $C$ " and " $\phi$ " for the overburden were selected using a correlation between friction angle and liquid limit(4) and assuming cohesion equal to zero.

The result of the computations indicated that when full uplift occurs, the stress at the base of the pier would be 2.7 KSF rather than 25 KSF. Any analysis which accounts for pier load will be performed using both stresses. Figure 4.1 shows load in the pier shaft versus

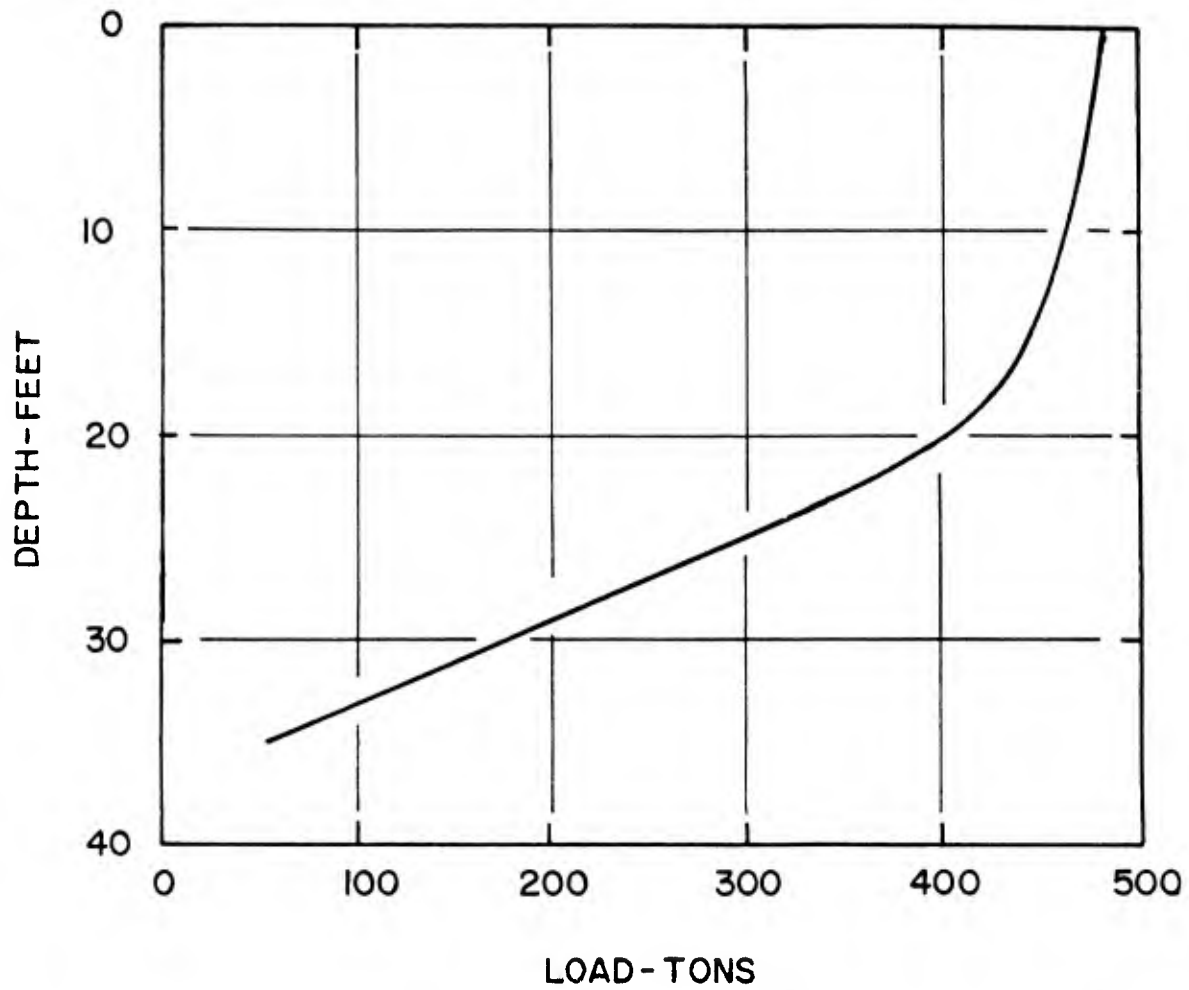


Figure 4.1 Pier shaft load versus depth for full uplift

depth and indicates the load taken up by the swelling soils adjacent to the pier shaft.

4.1.5 Final Pore Water Pressure Distribution(5). The final pore pressure distribution is very difficult to determine beneath a structure and very little appears in the literature concerning the subject. A number of assumed distributions can be used to bound the correct answer. Two distributions were assumed for this thesis. First it was assumed that all negative (suction) pore pressures were relieved and pore water pressure ( $U_w$ ) equals zero throughout the active zone. This is a conservative assumption that results in larger heave values being calculated but this distribution is unlikely to occur. The second distribution, Hydrostatic II, is described by the equation:

$$u_w = u_{wa} + \gamma_w (Z - X_a) \text{ where} \quad \text{Eqn 4.2}$$

$u_w$  = Pore Water Pressure at Z

Z = Depth where pore water pressure is to be computed

$u_{wa}$  = Known pore water pressure at depth  $X_a$

$\gamma_w$  = Unit weight of water

These distributions are required to use McClelland and Sullivan's method and the computer program HEAVE. For McClelland and Sullivan's method,  $u_{wa}$  was set equal to the difference between the expansion and overburden pressures. In all cases  $X_a$  equals 60 feet which is the depth to the bottom of the active zone 20 feet below the pier bottom. It is assumed that the initial and final pore water pressures at 60 feet are

equal and that the final pore water pressure decreases as described by the above equation from that point.

The mechanical model in the program HEAVE follows a similar procedure while the input soil suction data are used in the suction option.

4.2 van der Merwe's Correlation. This technique was directly applied to predict the heave that would occur from 40 feet to 60 feet. Heave of 0.08 inches was computed.

4.3 Vijayvergia and Ghazzaly's Correlation. Direct application of these equations to analysis of a drilled pier foundation was not considered appropriate because the percent swell correlations do not consider overburden pressure or additional structural pressure. These are significant factors in analyzing the performance of a drilled pier foundation. All of the tests used to develop the four correlations were conducted on samples taken within 10 feet of the ground surface consequently the percent swell equations are good for cases with minimal overburden pressure and structural pressure, i.e. slab-on-grade foundations. To use this method to analyze a drilled pier foundation a curve like the one shown in Figure 4.2 was constructed assuming that the percent swell calculated from the correlation is at zero pressure and that at the calculated swell pressure the percent swell is zero. The percent swell at the overburden plus additional structural pressure can then be computed using ratios. This type analysis was performed using Equation 2.3 and 2.5 (Water Content Correlations) and Equation 2.4 and

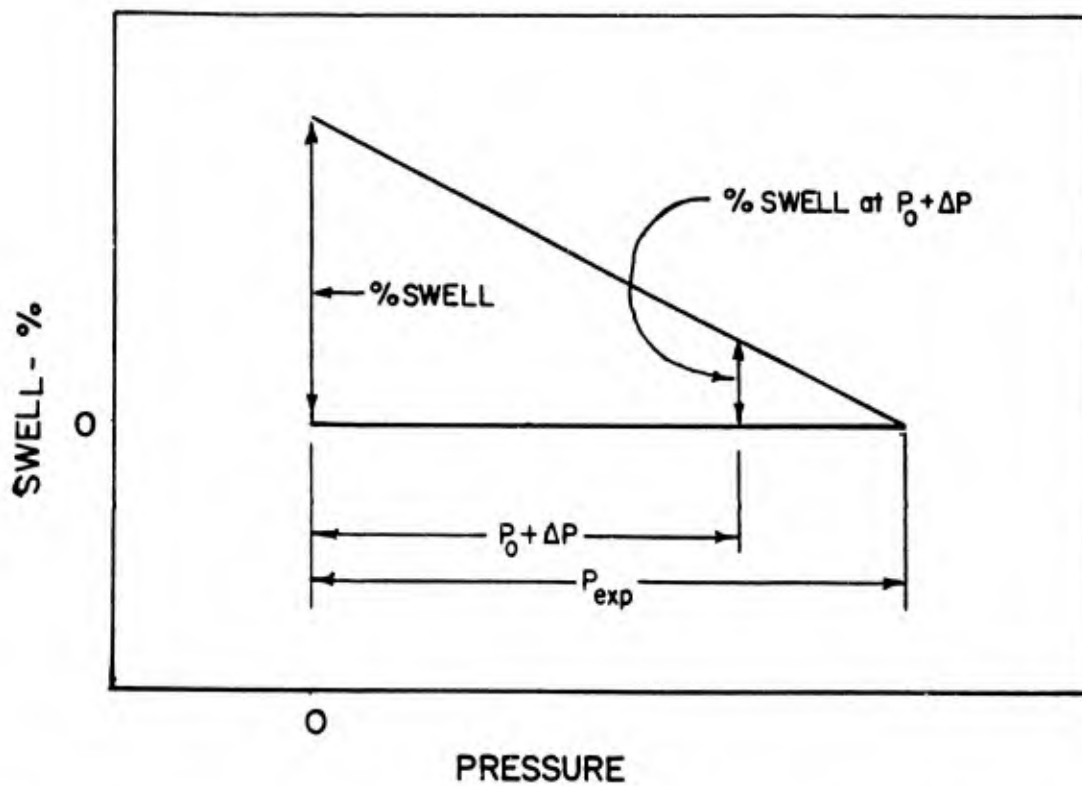


Figure 4.2 Analysis of results using Vijayvergia and Ghazzaly's correlation

2.6 (Dry Density Correlations). The predicted heave is shown in Table 4.1 for the assumed base pressures of 25 ksf and 2.7 ksf.

TABLE 4.1

RESULTS FROM VIJAYVERGIA AND GHAZZALY'S CORRELATION

	<u>Heave (inches)</u>	
	25 ksf	2.7 ksf
$w_o$ correlation	0	0
$\gamma_d$ correlation	0.42 in	2.9 in

The advantages of this method are its simplicity and the relatively inexpensive testing required. However, the coefficients of correlation of 0.7 are low. Also, despite the statement that the tests used to develop the correlations have wide geographic coverage, the bulk of the tests (80%) come from Texas and are concentrated along the Gulf Coast.

This is particularly important since soil properties are a function of the geologic origin of the parent rock the soil was formed from, chemical composition of the soil, climate, location of ground water and so on, all of which are unique to a particular area. Sound engineering judgement is required before extending empirical correlations outside the areas for which they were developed.

4.4 McClelland and Sullivan's Method. Three swell pressure tests were analyzed assuming 25 ksf and 2.7 ksf at the pier bottom using both assumed final pore water pressure distributions. The results are shown in Table 4.2 with heave in inches.

TABLE 4.2

RESULTS FROM McCLELLAND AND SULLIVAN'S METHOD

Test	<u>Heave (inches)</u>			
	$q_0 = 25.0$ ksf		$q_0 = 2.7$ ksf	
	Case 1	Case 2	Case 1	Case 2
1	0.125	0	0.752	0
2	0.032	0	0.400	0
3	0.0	0	0.272	0

## Notes:

Case 1 =  $U_w = 0$  (Saturated Model)

Case 2 =  $U_w a + \gamma_w (Z - X_a)$  (Hydrostatic II Model)

This method is a relatively straightforward analysis technique with easily determined input except for selection of the final pore water pressure distribution which according to the writers "requires considerable judgement in some cases." The technique attempts to account for pore water pressure effects and if the sample is representative, other factors such as density, in situ water content, etc. will be indirectly accounted for.

4.5 Corps of Engineers Method. Three consolidation expansion tests were analyzed assuming 25 and 2.7 ksf at the pier bottom. The results, in inches are shown in Table 4.3.

TABLE 4.3

## RESULTS FROM THE CORPS OF ENGINEERS METHOD

Test	<u>Heave (inches)</u>	
	$q_0 = 25 \text{ ksf}$	$q_0 = 2.7 \text{ ksf}$
1	0	0.541
2	0	0.126
3	0	0.571

This method is also very straightforward and analysis is simple. It does not account directly for final pore water pressure but assumes that it equals zero and, assuming all other conditions are equal, should result in higher heave predictions than McClelland and Sullivan's method. If desired, the pore water pressure could be directly considered using the same approach as McClelland and Sullivan. An additional advantage of this testing technique is that consolidation characteristics are also determined.

4.6 Computer Program HEAVE. Predictions using the mechanical and suction models were performed with both final pore water distributions.

4.6.1 Input Data. Selection of the input soils data was based on looking at all of the available laboratory data and picking an average value for each of the strata. The input soils data are summarized in Table 4.4. The pore water pressure distributions used are the same ones discussed in paragraph 4.1.5.

TABLE 4.4  
INPUT DATA FOR PROGRAM HEAVE

<u>Property</u>	<u>Overburden 0'-20'</u>	<u>Upper Primary 20'-40'</u>	<u>Lower Primary 40'-60'</u>	<u>Source</u>
$G_s$	2.65	2.65	2.65	Assumed
$W_o$	18	21	20	Fig. 3.4
$e_o$	0.830	0.560	0.530	Consol-Exp Test
$C(TSF)$	1.5	2.5	7.7	Q-Test
$\phi$	0	0	0	Assumed
$K$	1.9	2.5	2.5	(1)
$P_{exp}(TSF)$	1.5	3.0	4.5	Consol-Exp Test
$C_s$	0.05	0.05	0.03	Consol-Exp Test
$C_c$	0.23	0.08	0.05	Consol-Exp Test
$A(TSF)$	3.508	4.873	4.873	Fig. 4.3
$B$	0.104	0.168	0.168	Fig. 4.3
$\alpha$	0.33	0.33	0.33	(2)
$PI$	52	43	35	Fig. 3.4

(1) Calculated using  $\phi$  from direct shear test or  $\phi$  from liquid limit vs  $\phi$  from direct shear correlation<sup>2</sup>

(2) From personal conversation with Dr. L.D. Johnson, WES.

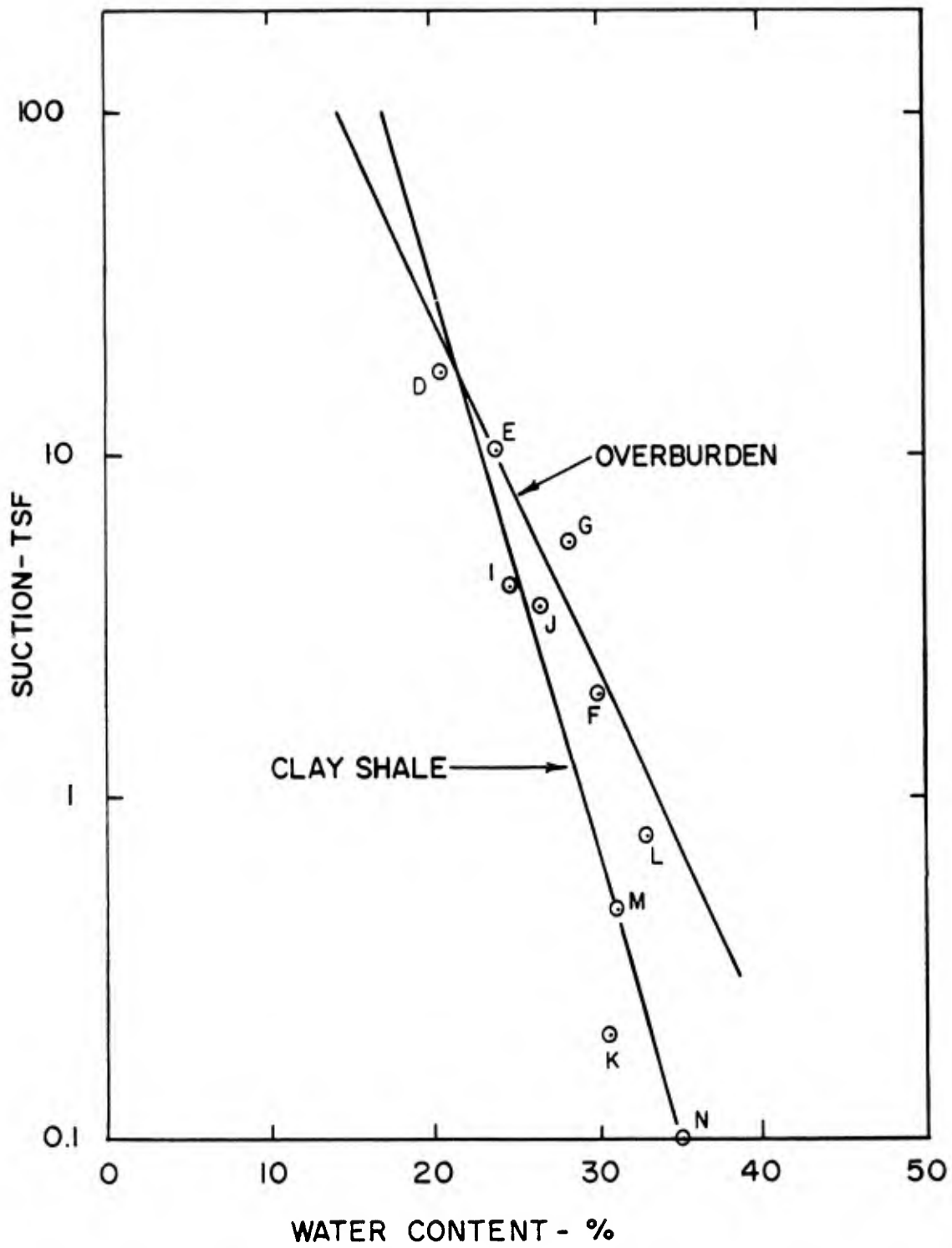


Figure 4.3 Determination of soil suction

The program has an option to make multiple runs using the same soils input but varying pier geometry so all three piers were analyzed instead of just analyzing pier H-18. The program also takes into account uplift along the pier shaft so the case with a 2.7 ksf loading at the pier base was not needed.

4.6.2 Suction Model Results. Results using the suction model are shown in the Table 4.5.

TABLE 4.5

RESULTS FROM PROGRAM HEAVE, SUCTION MODEL

<u>Pore Pressure Profile</u>	<u>Pier Movement - Inches</u>		
	<u>H-16</u>	<u>H-18</u>	<u>F-19</u>
Saturated	8.20	8.22	8.78
Hydrostatic II	-0.16	-0.13	-0.07

<u>Pore Pressure Profile</u>	<u>Load at Pier Base - Tons</u>		
	<u>H-16</u>	<u>H-18</u>	<u>F-19</u>
Saturated	296.9	268.4	140.4
Hydrostatic II	296.9	268.4	140.4

The movements predicted by the suction model assuming a saturated profile are well in excess of what would be considered acceptable. The program assumes all of the heave occurs in the vertical direction while

in reality some will occur laterally. At most this would reduce the vertical heave to approximately 2.8 inches, if the soil expanded equally in all three directions. This is also an excessive amount of movement but it represents the worst condition that could occur.

The suction model using the Hydrostatic II profile predicted settlement under all of the piers. The settlement is well within acceptable limits of 1 inch.

The load at the bottom of the piers was not affected by the assumed final pore water pressure distribution. Piers H-18 and H-16 have roughly the same load while pier F-19 was considerably less. A closer examination of the pier geometry and loading was made and the results are summarized in Table 4.6.

TABLE 4.6

PIER GEOMETRY AND LOADING

	<u>H-16</u>	<u>H-18</u>	<u>F-19</u>
Shaft Diameter (In)	36	30	30
Bell Diameter (In)	90	84	72
$D_b/D_s$	2.5	2.8	2.4
Design Load (Tons)	552	481	353
Load at Bell (Tons)	296.9	268.4	140.4
% at Bell	49	56	40

The relation between the percentage of column load at the bell and the bell diameter/shaft diameter ratio should be noted. The higher

$D_b/D_s$  the higher the percentage of the column load at the bell. This is because a high  $D_b/D_s$  ratio mean the pier has the minimum shaft diameter for the bell size. The larger the bell the more load that can be applied yet with the smaller shaft the expansive soil has less area to act against and the large bell is able to resist more uplift.

Comparison of H-18 and F-19 would seem to bear this out. Comparison of H-16 and H-18 is also interesting. Pier H-18 would be expected to heave more than pier H-16 since it has a smaller column load applied at the bell, yet H-18 heaves only 0.02 inches (0.25%) more than H-16. The additional resistance of the bell and the smaller area of the shaft appear to have combined to lessen the heave.

4.6.3 Mechanical Model Results. Results using the mechanical model are shown in the tables below.

TABLE 4.7

RESULTS FROM PROGRAM HEAVE, MECHANICAL MODEL

<u>Pore Pressure Profile</u>	<u>Pier Movement - Inches</u>		
	<u>H-16</u>	<u>H-18</u>	<u>F-19</u>
Saturated	-0.35	-0.34	0.10
Hydrostatic II	-1.60	-1.58	-1.22

Load at Pier Base - Tons

Pore Pressure Profile

	<u>H-16</u>	<u>H-18</u>	<u>F-19</u>
Saturated	296.9	268.4	140.4
Hydrostatic II	296.9	268.4	140.4

Pier movements using the saturated profile are all within acceptable limits with piers H-16 and H-18 settling slightly and F-19 heaving slightly.

Pier movements using the Hydrostatic II model were all settlement and slightly larger than a normally accepted 1 inch settlement. The differential movement however is 0.4 inches which is normally acceptable.

The loads at the pier base were the same as for the suction model and the same conclusions apply.

4.6.4 Further Analyses. The principle advantage of computer programs is being able to analyze a problem under a variety of conditions. By varying one parameter while holding the others constant the importance of that parameter can be determined. Also a solution can be bounded by varying a parameter from its maximum to minimum value.

Three parameters were selected for further evaluation. They are initial water content, lateral earth pressure coefficient and compressibility factor, alpha. These parameters were investigated using the suction model and the saturated pore water profile since this particular

combination yielded the most surprising results when compared to the remaining prediction. The results of these analyses are shown graphically on Figure 4.4 through 4.6.

Figure 4.4 shows initial water content with respect to movement. A one percent change in moisture content results in a 0.12 foot (1.4 inch) difference in heave. Selection of initial moisture content, especially near the surface, can be difficult. It is subject to errors due to sampling techniques and moisture loss/gain when the sample is taken and tested due to exposure to the open atmosphere. Consequently the samples should be handled carefully in order to minimize changes in water content so the initial moisture content can be accurately determined.

Figure 4.5 shows lateral earth pressure coefficient with respect to movement. Increasing the earth pressure coefficient decreases the amount of heave but the amount of the decrease becomes less as the coefficient increases so that at some point increasing earth pressure coefficients have no effect.

Figure 4.6 shows the compressibility factor alpha with respect to movement. Two plots are shown, one for an initial water content of 18% and the other for 30%. They indicate that as alpha increases the soils expansive potential increases. This is obvious for the 18% water content. The 30% water content shows that while the soil settles the settlement is offset more by heave when alpha is 1.0 rather than 0.33.

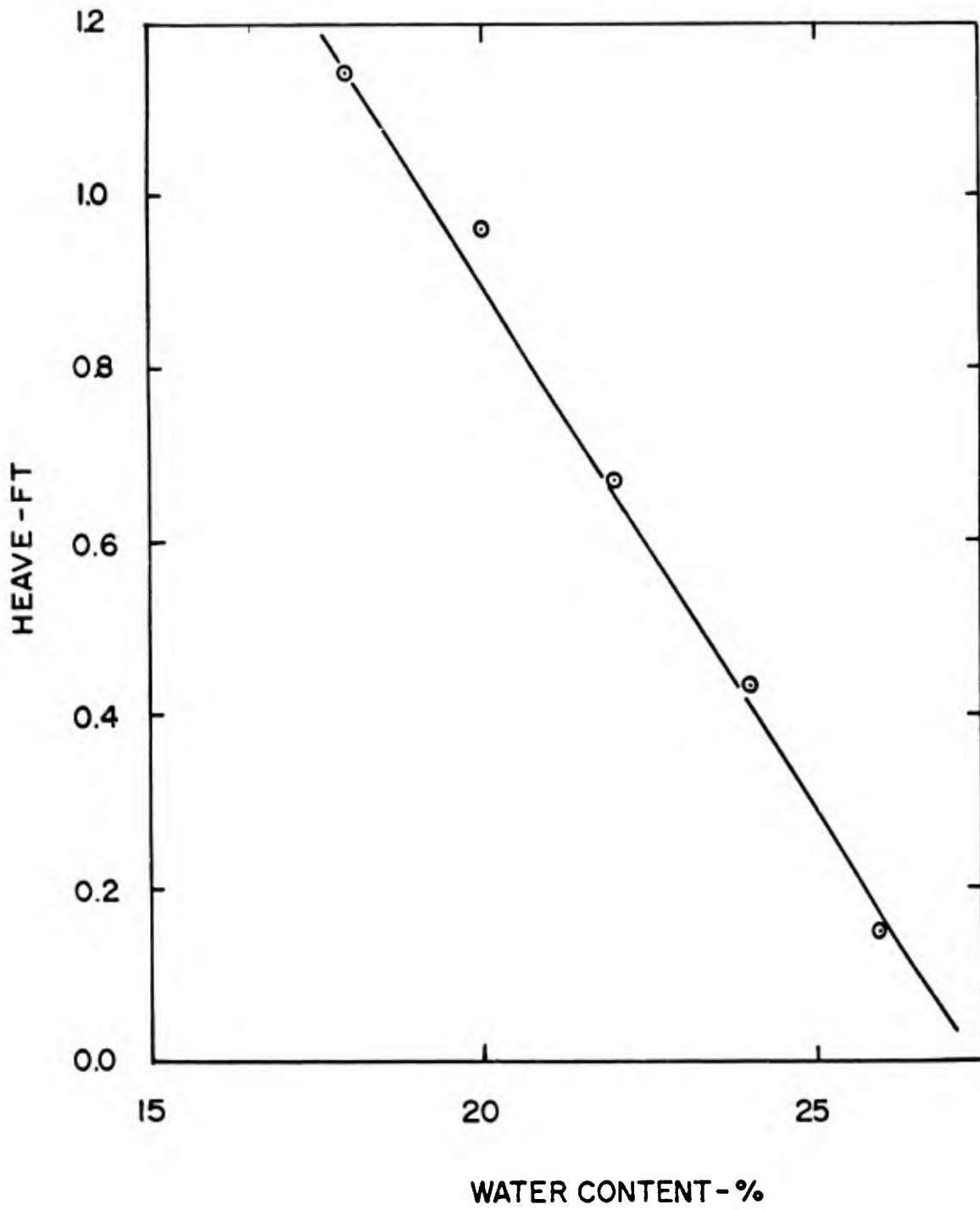


Figure 4.4 Water content versus heave

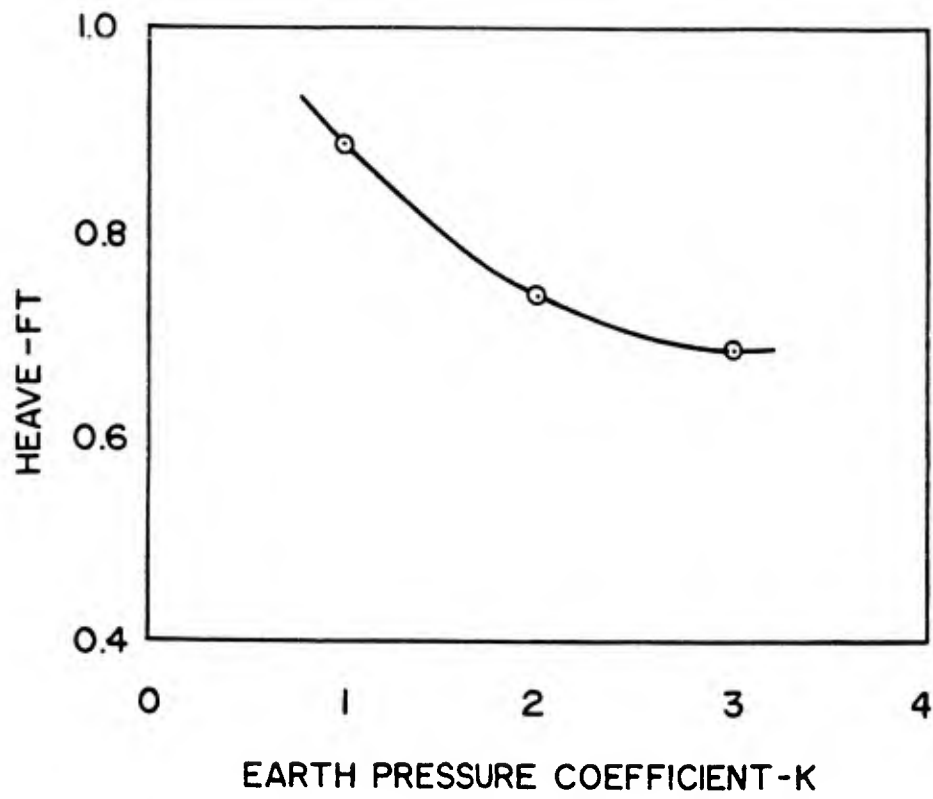


Figure 4.5 Earth pressure coefficient versus heave

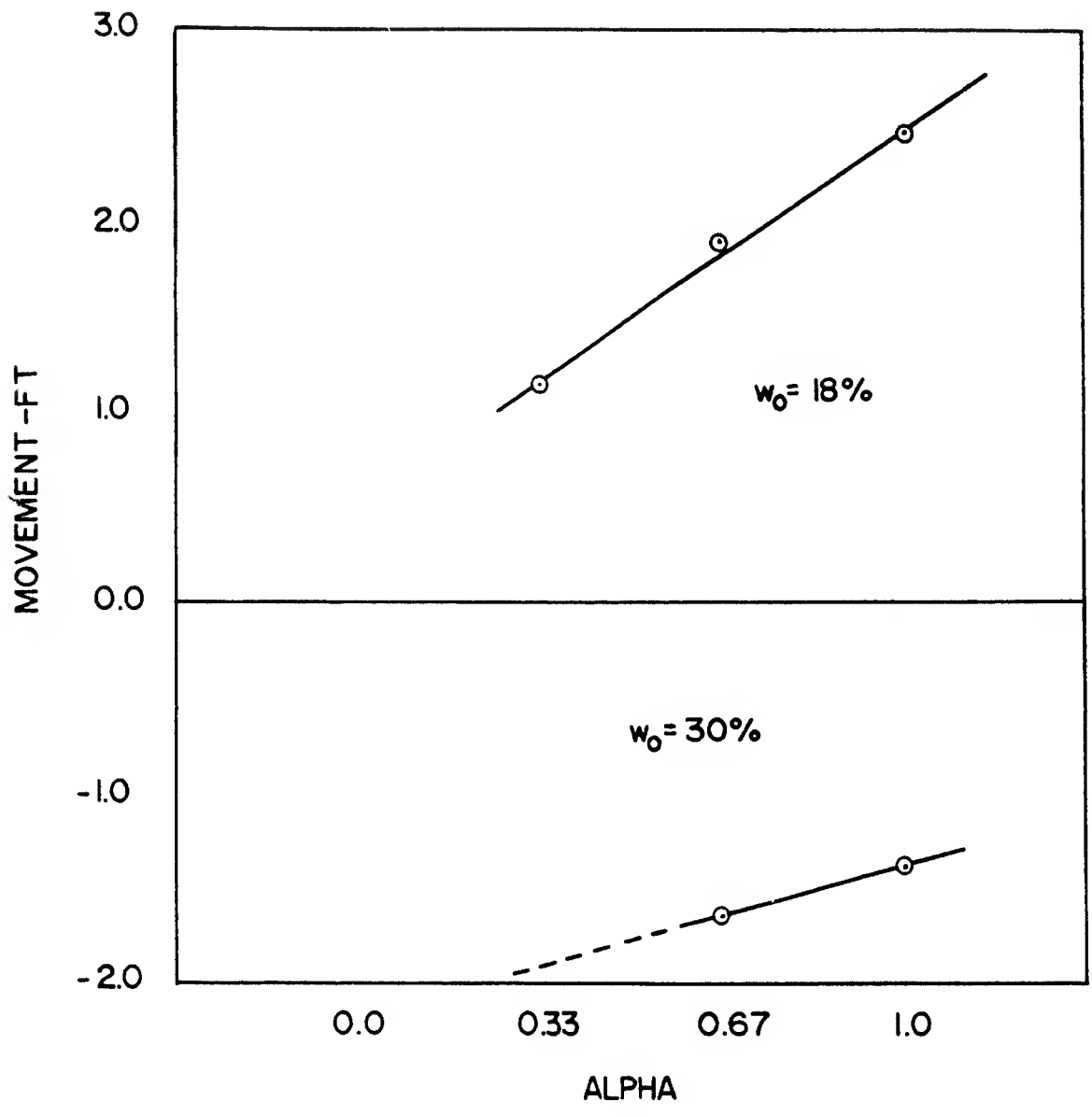


Figure 4.6 Alpha versus movement

Another interesting fact is that the slope is steeper when heave occurs than when settlement occurs. This is probably related to the fact that the moisture deficiency of a soil at 30% is less than one at 18%. This indicates that the soil will heave less and the soil becomes moisture satisfied more rapidly and expands less with a larger initial water content.

The results of these analyses indicate that the parameters in order of importance are initial water content, alpha and earth pressure coefficient, with the initial water content being the most important.

## CHAPTER 5

### ANALYSIS OF INSTRUMENTATION

5.1 Free Standing Benchmarks. Four free standing benchmarks were installed as detailed in Chapter 3. The deepest one, FSH-4, has been used as the datum to measure the movement of the three remaining free standing benchmarks as well as the grade beam benchmarks. Consequently, it is assumed that FSH-4 has not moved.

The free standing benchmarks have been surveyed three times. Once when they were installed (Aug 70) to establish their initial elevation, again 11 months later when initial elevations for the grade beam benchmarks were established and finally in May 82 for preparation of this report.

FSH-1 was founded 2 feet below the ground surface in clay. It has shown downward movement on both subsequent surveys. Since these surveys were performed during the summer the downward movement was probably due to shrinkage of the surface soils which is characteristic of expansive soils.

FSH-2 and FSH-3 have both shown upward movement. FSH-2 is located 12.3 feet below the ground surface in a gravel stratum while FSH-3 is located 19.0 feet below the ground surface and 3.8 feet into primary material. These benchmarks have experienced roughly equal movements with both of them moving upward slightly more than 0.7 inch in 12 years.

These movements are probably due to an inflow of water resulting in expansion of the clay shale primary material. Typically, a gravel layer is encountered at the overburden-primary contact and a perched water table exists in the gravel. The perched water table provides a source of water for the moisture deficient clay shale. The 0.7 inch heave in the gravel (FSH-2) is probably due to a 0.7 inch heave in the upper primary which is also reflected by (FSH-3). This may represent a long term effect where the upper primary material is continually expanding under natural conditions, assuming the benchmarks have not altered these conditions.

FSH-4 is assumed not to have moved. This benchmark is founded 45 feet below the ground surface and 32 feet into the primary clay shale. This benchmark is below the zone of seasonal moisture change, below any active zone due to the perched water table and should therefore be in a moisture stable material in its in situ condition.

Figure 5.1 shows a plot of movement versus time for the free standing benchmarks.

5.2 Grade Beam Benchmarks. Thirty-seven benchmarks were installed on the building when the grade beams were constructed. Initial elevations of the benchmarks were established in June 1971 with subsequent surveys in January 1972, January 1973, and May 1982.

The general trend of movement was downward (settlement) from June 1971 to January 1972 and then upward (heave) from January 1972 to May

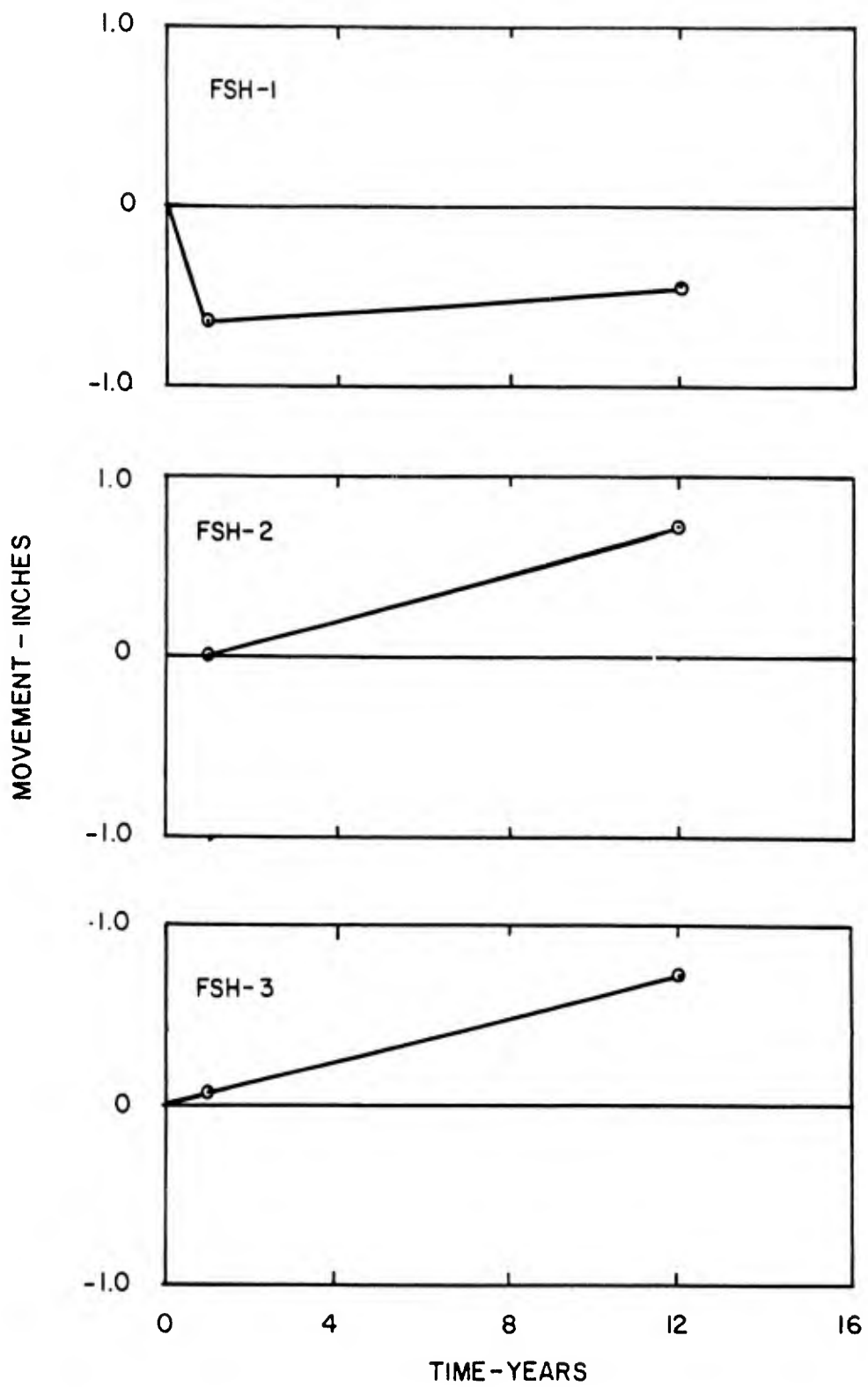


Figure 5.1 Movement versus time-free standing benchmarks

1982. As of the May 1982 survey, 21 of the benchmarks are above their original elevation, two are at their original elevation and 14 are below their original elevation. Comparison of the January 1973 survey, near the end of construction, and the May 1982 survey shows that 26 of the benchmarks have moved upward. Of the remaining 11 benchmarks, six are within the survey error of showing no movement or upward movement and the other five have gone down only 0.007 to 0.010 feet. All 11 of these benchmarks are located on the 3 story portion of the building and are therefore the most heavily loaded.

A plan view of the MFSS showing movement contours as of May 1982 is shown on Figure 5.2. Plots of movement versus time are shown on Figure 5.3. Figure 5.3a shows the movement of the benchmarks experiencing the greatest upward and downward movement. Figure 5.3b shows the movement of the benchmarks located near piers H-16 and H-18. Figure 5.3c shows the movement of the benchmarks located near pier F-19.

5.3 Strain Gages. Three piers under the 3 story part of the MFSS were instrumented with five strain gages each. Each of the gages were read with the reinforcing cage vertical in the pier shaft prior to placement of the concrete to establish a zero load reading. Each of the gages were regularly checked from October 1970, when the piers were constructed, until January 1973, when readings were stopped. Another reading was made in July 1982 in order to prepare this thesis.

All of the gages reacted in a very similar manner during the initial readings. As soon as the concrete was placed in the pier shaft the



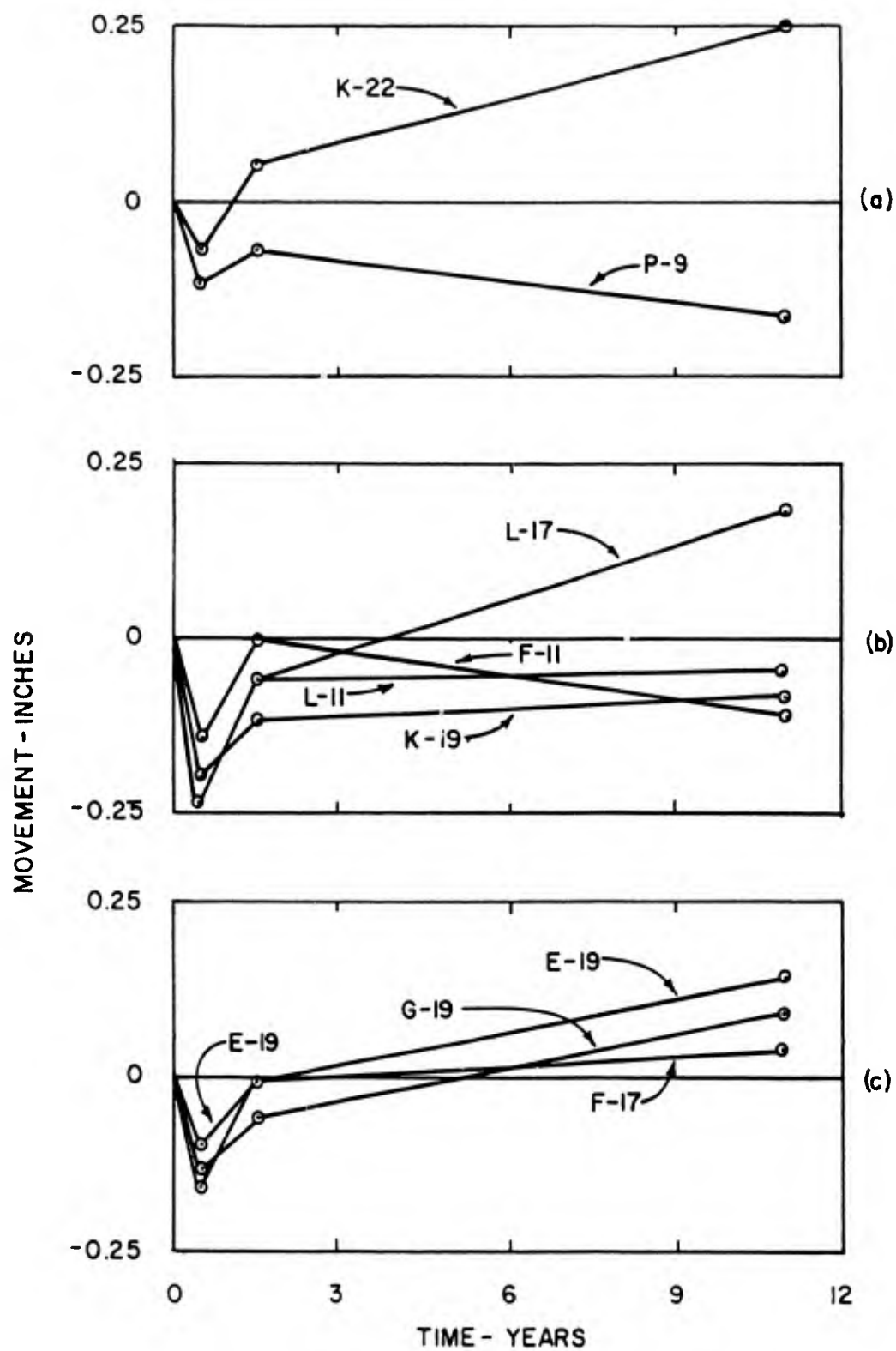


Figure 5.3 Movement versus time-gradebeam benchmarks

gages immediately showed compression due to the weight of the concrete on the reinforcing cage. Within a matter of hours, presumably when the concrete began to set, the gages began indicating tension. The strain gages showed a typical tensile strain of about 50 micro inches per inch from the day after the piers were constructed until the structural loads began to be applied to the piers approximately 7 months later. The cause of this tensile load is not certain but similar behavior was observed at the Lackland AFB Test Pier site in 1966 and 1967<sup>(15)</sup>. Once the structural load was applied all of the gages indicated compression and the load in the pier shaft decreased with depth, as would be expected, indicating some of the load was being reduced due to skin friction along the side of the pier.

To further analyze the pier performance the strains measured by the strain gages were converted to stresses and loads. These analyses will be covered in greater detail in the following paragraphs.

5.3.1 Initial Analyses. Prior to beginning an analysis of the strain gage data, a number of assumptions were made. They are listed below.

1. Modulus of elasticity for steel =  $E_s = 30 \times 10^6$  psi
2. Modulus of elasticity for concrete =  $E_c = 3.3 \times 10^6$  psi in accordance with the ACI Code, paragraph 8.3(2)
3. In tension all of the load is carried by the steel

4. In compression the load is carried by the steel and the concrete and was determined using the equation

$$P = \sigma_s A_s + \sigma_c A_c \quad \text{Eqn 5.1}$$

where:

$P$  = Compressive Load

$\sigma_s$  = Stress in the Steel

$A_s$  = Area of Steel

$\sigma_c$  = Stress in the Concrete

$A_c$  = Area of Concrete

5. In compression the strain in the steel, as measured by the strain gages, is equal to the strain in the concrete.
6. Any change in load between strain gages is due to skin friction developed between the pier shaft and the surrounding soil.
7. Hooke's Law is valid for the steel and concrete.

Using the measured strain values, corresponding stresses in the steel and concrete were computed, and the load in the pier shaft was determined. The readings taken prior to July 1982 appeared reasonable and followed a pattern that would be expected. The pattern indicated the maximum load was at the top of the shaft and the load in the shaft decreased with depth due to skin friction. The July 1982 readings showed the same load pattern except the load at the top of the shaft was 1.6 to 3.4 times the computed column load. Also for pier H-16 the change in load between the first and second gage which was presumably reduced by skin friction would require a soil cohesion of 45 tsf.

This is well in excess of any normally encountered value. Some of the increase in shaft load could be explained by the pier heaving with respect to the adjacent piers and consequently picking up some of their load. This could not account for a 3-fold increase nor did a 45 ksf cohesion value seem reasonable. Therefore, a reassessment of the assumptions seemed in order.

The strain gages measure the strain in the steel. Therefore, the strain, corresponding stress and the load carried by the steel is known exactly. The strain, stress and load in the concrete are assumed based on the strain in the steel. Barring a defect in the pier shaft or a failure of the shaft, the strain in the concrete must be the same as in the steel. Neither a shaft failure or defect seemed likely. A defect in the pier would have been detected by earlier readings and a failure of the shaft did not seem likely based upon the good condition of the building and the loads in the remainder of the pier shaft. If a mechanism for transferring stress, in reinforced concrete under load from the concrete to the steel could be found, the high loads could be explained. Creep is such a mechanism.

5.3.2 Creep of Reinforced Concrete. Creep has a dual definition. It is defined as "a deformation occurring under, and induced by, a constant sustained stress, and a relaxation which is a decrease in stress with time under a constant deformation (12)." Stated another way, "creep, in general, tends to relieve stress in concrete, especially when

reinforced(14).” This is the situation encountered when trying to analyze the strain gage data. The stress in the concrete is considerably less than what is indicated by the strain gage data using the assumptions outlined in the previous section.

Creep in concrete is affected by a large number of factors which include the water-cement ratio, aggregate type, age at loading and curing conditions. The two factors of primary interest in analysis of the strain gage data relate to curing conditions. They are relative humidity and to a lesser extent temperature.

“In the case of temperature, it is the temperature of the concrete itself that affects creep but of course, beyond the initial period of hydration and excepting mass concrete, the ambient temperature controls the temperature of the concrete. The relative humidity of the surrounding medium has a more direct environmental influence on creep, which is affected by the drying of the concrete under load. The influence of relative humidity is large, for at a relative humidity of 50 percent, creep may be 2 to 3 times greater than at a relative humidity of 100 percent(12).” The affect of temperature may be very minor since research has shown that between 68°F to 136°F temperature did not affect creep of concrete which had dried out. This is the case under normal construction conditions. Research conducted on reinforced columns to investigate the effects of relative humidity is summarized in Table 5.1 on the next page.

TABLE 5.1

## UNIT STRESSES IN REINFORCED CONCRETE COLUMNS

Nominal strength of concrete at 28 days, psi	Axial steel ratio, %	Total load applied to column lb	Unit stress, psi							
			At time of application of load		1 year under load		3 years under load		5 1/2 years under load	
			Steel	Con-crete	Steel	Con-crete	Steel	Con-crete	Steel	Con-crete
Columns stored in air of 50 percent relative humidity at 70°F										
2000	5.0	22,300	9,660	875	26,900	-20+	27,400	-50+	28,000	-75+
2000	1.9	14,200	6,540	610	34,800	60	35,700	45	37,100	15
4000	1.9	21,800	7,860	975	37,500	395	40,400	340	41,700	315
Columns stored under water at 70°F										
2000	5.0	19,200	7,200	810	10,050	665	10,890	620	11,400	590
4000	1.9	13,650	5,460	605	7,980	555	9,060	535	9,480	525
4000	1.9	20,600	7,320	925	10,590	865	11,670	840	12,120	835

†Age at loading, 28 days

+Minus sign indicates tension.

diameter of columns, 5 in.

Source: Reference 14, After Troxell, Davis and Kelly

The significant stress increase in the steel and decrease in the concrete at 50% relative humidity is of particular interest. Note that in one case the concrete went into tension. The comparative stability of stress at 100% relative humidity is also of particular interest. This indicates that creep is negligible at 100% relative humidity and that all of the initial analysis assumptions would be applicable.

To use this information to interpret the strain gage data, the curing conditions of the piers should be examined closely. The geometry of the piers is such that the top gage is at the ground surface and the second gage at least 7 feet below the ground surface. The top of the piers and thus the top gage was exposed to the weather for approximately 1 year. Consequently, the concrete around the top strain gage was subjected to variations in both temperature and humidity. The lower gages were sufficiently far below the ground surface that the soil is assumed to provide a temperature stable environment and be at or near 100% relative humidity. The attraction of the surrounding clay soils for water and the presence of free water in the gravel stratum insure 100% relative humidity. These curing conditions would result in concrete around the top gage that would experience significant creep while the lower gages would be in concrete which would not be as susceptible to creep.

Considering the above information the following additional assumptions were made.

(1) For strain gages 2 through 5 (those located below the ground surface) all of the previous assumptions are valid and creep is assumed to be negligible.

(2) For strain gage 1 at the top of each pier all of the previous assumptions are valid for the readings prior to July 1982 and creep effects were not significant for these readings.

(3) For strain gage 1 creep has become a significant factor in the July 1982 readings. The load in the pier shaft at gage 1 is assumed to be equal to the load at gage 2 and no load is taken out in skin friction between gages 1 and 2.

Using these assumptions the strain gage readings were reanalyzed and those results are presented in the next section.

5.3.3 Reanalysis of Strain Gage Data. One additional change was made during the reanalysis of the strain gage data. Rather than use the zero reading taken when the concrete was placed in the pier shaft a new zero equal to the average of the five readings taken prior to July 1971 was used. Apparently the curing process in concrete produced a tensile stress in the reinforcing steel and plots of load versus time for pier H-16 are shown on Figure 5.4 illustrate this. The adjusted zero reading better represents what has happened to the pier since the initial structural loads were applied.

The results of the reanalysis are shown graphically on Figures 5.5, 5.6, and 5.7. They show load versus depth at four different times for piers H-16, H-18, and F-19, respectively.

The 1971, 1972 and 1973 plots for pier H-16, Figure 5.5, show the increase in pier load due to construction of the superstructure. The

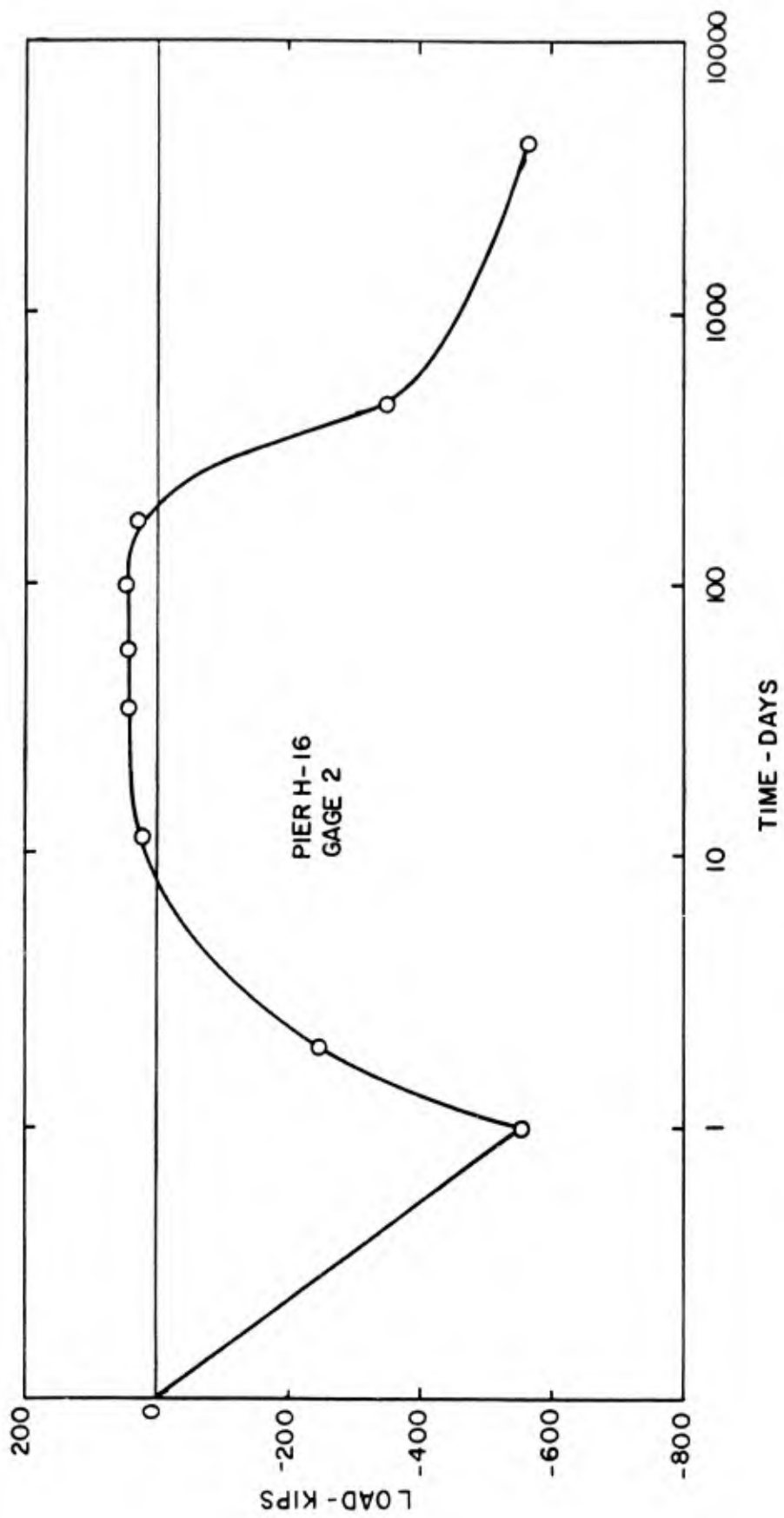


Figure 5.4 Load versus time

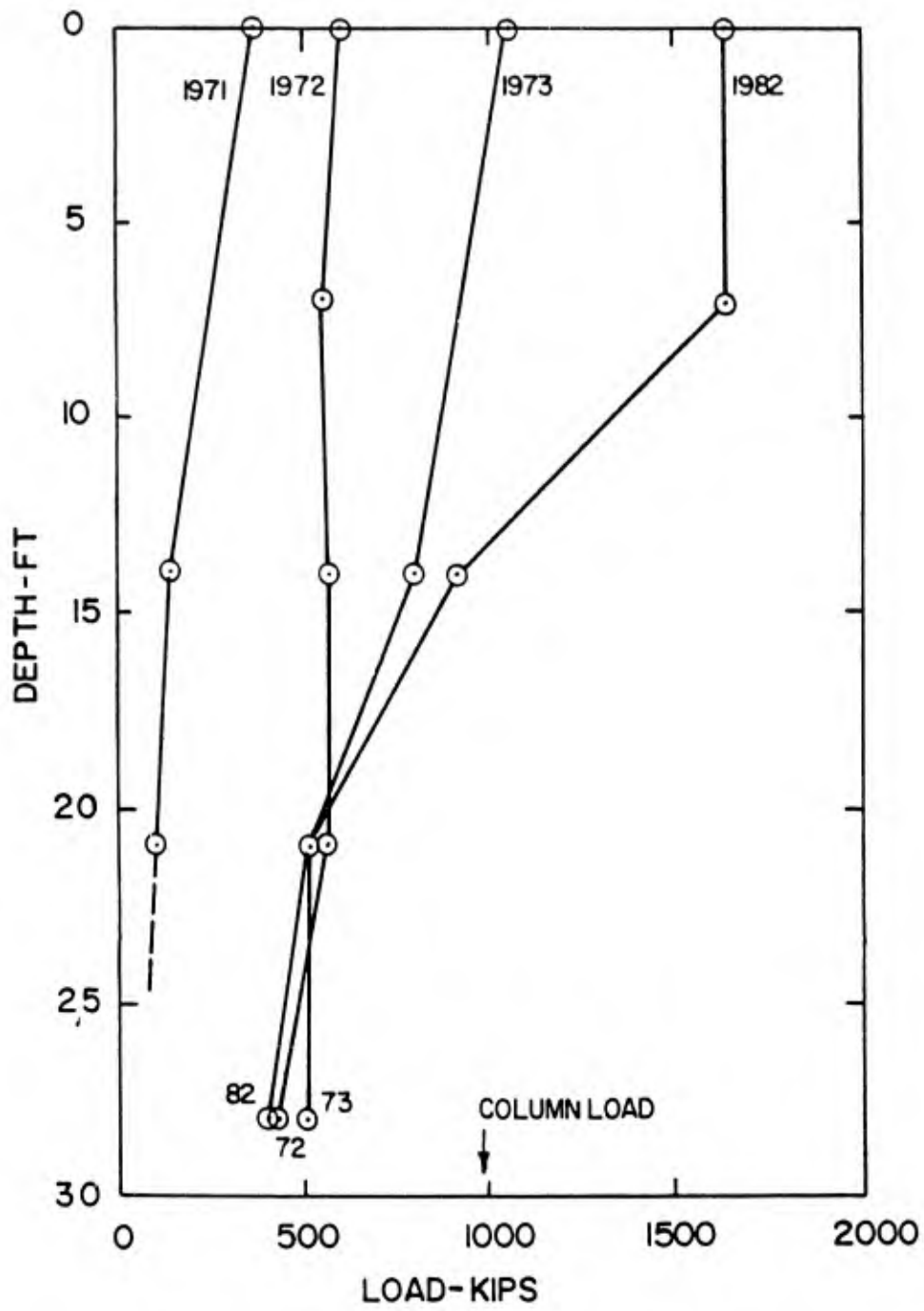


Figure 5.5 Load versus depth, pier H-16

loads are largest at the top of the pier and they tend to decrease with depth as would be expected. The load in 1973 at the top of the pier is approximately the computed design load. By 1982 the loads in the upper half of the pier increased significantly while the loads in the lower half remained relatively unchanged or decreased slightly. The increase in loading is probably due to heave of the clay overburden and upper zone of the highly jointed clay shale. This is the zone where most of the increase in load occurred. Heave in these materials should be expected. Free water was present in the gravel strata prior to construction of the piers but the ability of this water to move vertically was limited by the clay and clay shale above and below it. When the piers were constructed confinement of the free water in the gravel was ended because the pier-soil interface provided an avenue for the water to move vertically throughout the subsurface materials. Fissures in the clay overburden materials and joints in the clay shale further allowed the water to reach the materials adjacent to the pier which were previously isolated from the free water in the gravel. Once these moisture deficient materials had access to free water they swelled laterally, gripping the pier, and vertically, lifting the pier. The upward movement is more pronounced in the upper soils since there is less resistance due to overburden pressure. The more the soil moves upward the more load the soil can assume due to skin friction. Consequently, over a period of time the expansive soils take up more free water, swell and move upward more with respect to the pier shaft.

The near surface soils move the most therefore they assume more of the pier load via skin friction increasing the load at the top of the pier and decreasing the load at the bottom where movements are less.

The plots for pier H-18, Figure 5.6, show a trend similar to pier H-16 except the loads in 1982 at the top have not shown as large an increase. The increase in load is also probably due to heave of the overburden and upper primary materials.

The results from pier H-16 and pier H-18 need to be examined together in order to interpret their behavior. They are adjacent to each other and are connected by a common grade beam, therefore, they should have very similar subsurface conditions and the response of one will affect the other via the grade beam.

Both of the piers have shown a decrease in load at the bottom gage, Number 5, since the 1973 readings. This indicates two things. First, the clay shale under the pier bottoms has not expanded as much as the soils adjacent to the pier shaft have lifted the pier. This would cause an increase in load at the bottom of the shaft due to negative skin friction and compression of the concrete. Second, since the load has decreased, the load had to be taken out from above gage 5 which indicates heave of the soil adjacent to the shaft created uplift.

Gages 2, 3, and 4 in the two piers indicate loads equal to or in excess of those in recorded 1973 and, for a given year, an upper gage

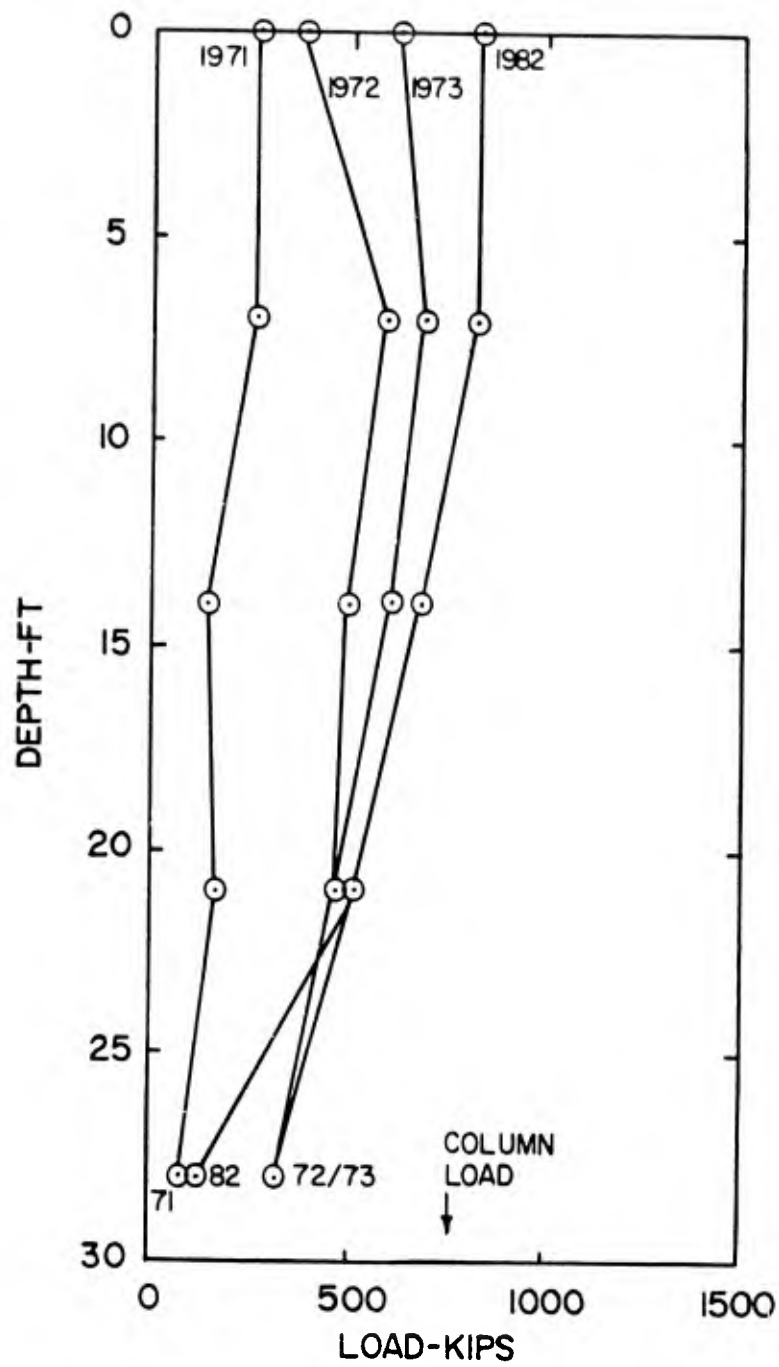


Figure 5.6 Load versus depth, pier H-18

indicates more load than a lower gage, i.e., gage 2 shows a higher load than gage 3. This is, also, indicative of swell adjacent to the pier shaft creating uplift. At any given time the upper soil stratum can swell more than the lower stratum when there is an increase in moisture content because there is less confinement by the overlying soils. At a given depth over a period of time the soil will be able to increase in moisture content, expanding further and creating more uplift.

The significant increase in load at the top of pier H-16 can also be explained. The load in the shaft has increased considerably over the 1973 readings and the load at the top is 65% larger than the computed design column load. Pier H-18 has shown much smaller increases in load in the pier shaft and the load at the top is only 9% larger than the computed design column load. Subsurface conditions at these two piers should be very similar, they are only 36 feet apart, however, pier geometry is not the same. Pier H-16 has a 36-inch diameter while H-18 has a 30-inch diameter, which means H-16 has 44% more surface area per linear foot of shaft than H-18. The expanding soils adjacent to the piers will have more surface area to react against at pier H-16 than at pier H-18, consequently, the loads will be larger in pier H-16. Further compounding the situation is that increased uplift will cause pier H-16 to move up with respect to pier H-18. This relative upward movement will cause some of the load carried by pier H-18 to be transferred, via the grade beam, to pier H-16.

The response of pier H-16 and pier H-18 can be summarized as follows. The clay shale below the pier bottoms has not expanded as much as the soils adjacent to the shaft. The overburden and upper weathered, jointed primary clay shale has expanded creating uplift along the pier shaft. The larger surface area of pier H-16 has caused it to carry much larger loads than pier H-18 and the relative upward movement of H-16 with respect to H-18 has caused H-16 to have some of H-18's load transferred to it which further increased the load in the shaft of H-16.

Pier F-19 is located at the perimeter of the MFSS, and an expansion joint passes over it. Based on the benchmark surveys this pier has moved upward approximately 0.15 inch. The strain gage measurements for this pier are very erratic and do not follow any recognizable pattern as with piers H-16 and H-18. Loads in the pier shaft are shown with respect to depth on Figure 5.7. The 1971, 1972, and 1973 readings show gage 2 with a larger load than gage 1 and gage 5 with a larger load than gage 4. This does not seem consistent with what was seen in the other piers and does not follow the expected pattern of decreasing load with depth. A clue to the erratic behavior may be found in gage 3. In 1971 it showed a small tension load and in 1972 it showed a small compressive load. In 1973 it showed a very large tensile load, well beyond the yield point of the steel. Finally, in 1982, the gage was completely inoperative. Possibly the pier failed in tension at gage 3 sometime between the 1972 and 1973 readings and if this has occurred, the leads to gages 4 and 5 may have been damaged. Uplift of the soil

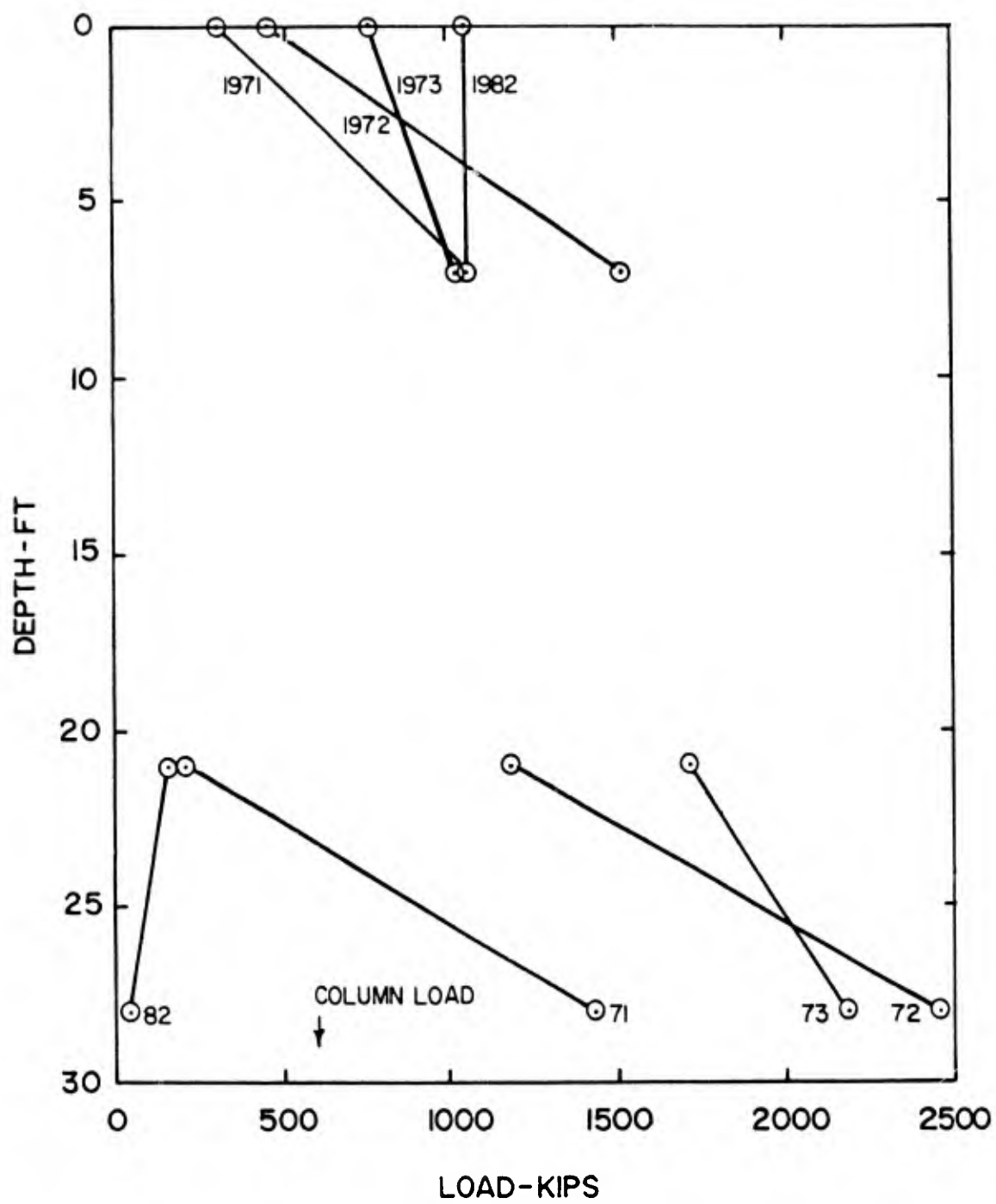


Figure 5.7 Load versus depth, pier F-19

around the upper part of the shaft could cause a high load at gage 2 which would be reduced by negative skin friction accounting for the lower load at gage 1. In any case the soil-shaft interaction as measured by the strain gages is inconsistent and only future readings may offer a clue to what is actually occurring at these locations.

5.4 Assessment of Building Performance. The MFSS has performed very well and inspection of the building showed no signs of cracking or other structural distress. The expansion joints show little visible relative movement and the maintenance personnel had no complaints that would indicate foundation problems.

The perimeter benchmark surveys indicate little net upward movement has occurred but the benchmarks are showing a definite trend of upward movement. Apparently the clay shale under the piers settled when initially loaded but within 1 year the piers began to move upward as expansion forces gripping the pier shafts overcame the forces causing settlement. Movements as of 1982 are well within the assumed allowable movement of 1-inch, however, the MFSS was completed in 1973 so only 9 years of its service life have elapsed. The movements in a 20-, 30-, or 50-year service life may exceed the 1-inch allowable.

The performance of the piers themselves, as measured by the strain gages, is somewhat ambiguous. Piers H-16 and H-18 have performed as expected. Loads have decreased with depth and as time has elapsed the loads in the upper part of the shaft have increased due to expansion of

the soils adjacent to the shaft while loads at the bottom of the shaft have decreased due to the expansion. Apparently expansion of the clay shale below these shafts has not been appreciable.

The performance of pier F-19 leaves more questions than answers. Perhaps further observation and monitoring of the instrumentation will answer these questions. Overall the piers have apparently performed very well since the MFSS is functioning satisfactorily which is the final criteria in establishing success or failure of the foundation.

## CHAPTER 6

### PREDICTED PERFORMANCE VERSUS ACTUAL PERFORMANCE

6.1 General. The previous two chapters have dealt with predicting the performance of the MFSS using techniques which have been presented in the literature and assessing the actual performance of the MFSS based on data collected from benchmarks and strain gages. Comparison of the predictions with the actual measurements should provide some insight into the ability of each technique to predict heave of a drilled pier foundation. One thing to bear in mind when making these comparisons is that each method predicts the movement that may take years or decades to occur, while the actual movements are based on only 9 years of observation.

Table 6.1 lists the movement predicted by each method and the actual movements measured by the level surveys.

6.2 van der Merwe. At first glance this method appears to have correlated very well. The prediction of 0.08 inches is well within the range of movements measured and is within one standard deviation of the average movement. When evaluating this result, it should be remembered that the analysis technique does not consider structural loads applied to the pier. The prediction would be the same for a pier designed for 25 ksf end bearing or 2 ksf end bearing assuming similar conditions. Since the expansion pressure of the clay shale below the pier is approximately 9 ksf, it is readily apparent that a pier with 2 ksf end

TABLE 6.1

## SUMMARY OF PREDICTED AND MEASURED MOVEMENTS

## PREDICTIONS

 $q_0=25 \text{ ksf}$  $q_0=2.7 \text{ ksf}$ 

Method	$q_0=25 \text{ ksf}$		$q_0=2.7 \text{ ksf}$	
	$U_w=0$	$U_w=\text{Hydro II}$	$U_w=0$	$U_w=\text{Hydro II}$
van der Merwe	0.08	0.08	0.08	0.08
Vijayvergia & Ghazzaly ( $W_0$ )	0	0	0	0
Vijayvergia & Ghazzaly ( $\gamma_d$ )	0.42	0.42	2.9	2.9
McClelland & Sullivan	0.05	0	0.48	0
Corps of Engineers	0	-	0.41	-
HEAVE (Suction Model)	8.2*	-0.13*	-	-
HEAVE (Mechanical Model)	-0.34	-1.58	-	-

\*N = 1

Number in parenthesis are the total heave.

## MEASUREMENTS

Average Movement	0.022 in $\pm$ 0.102	(-0.080 to 0.124)
Range	-0.168 to	0.252

bearing would experience considerable movement. The conclusions to be reached is not that this technique is bad but rather it was developed with slab on grade foundations in mind, not drilled piers, and should be used only for predicting movements of slabs on expansive soils.

6.3 Vijayvergia and Ghazzaly. The correlations developed by Vijayvergia and Ghazzaly could not be directly applied to a drilled pier foundation but instead were used essentially to construct a plot similar to a swell pressure test and analyzed accordingly. The water content correlation predicted no heave would occur while the dry density correlation predicted either 0.42 inches or 2.9 inches of movement depending upon the assumed end bearing pressure. The 0.42 inches and 2.9 inches represent an upper and lower limit to the amount of heave that might occur. Since the 25 ksf end bearing is the most that can occur, the heave will certainly be in excess of 0.42 inches but less than 2.9 inches. The next question is which correlation is correct. Vijayvergia and Ghazzaly state that the water content correlation is more accurate since water content can be measured more accurately than dry density. However, it is difficult to ignore the predictions using the dry density correlations since it is considerably larger. The answer to this is the same as with van der Merwe's correlation. Vijayvergia and Ghazzaly's correlations were specifically developed for use with slab on grade foundations. All of the samples used to develop the correlations were obtained from less than 10 feet below the ground surface; therefore extension of these results to depths in excess of 10 feet, where over-

burden pressure becomes more of a factor, probably was not envisioned by the writers. This method should be used for shallow foundations only and not drilled piers.

6.4 McClelland and Sullivan. This method appears to have correlated very well. No heave was predicted for the Hydrostatic II profile while movements up to 0.5 inch were predicted for the saturated profile. Since the 0.5 inch of movement represents an upper limit of the expected movement, the measured maximum heave of 0.25 inch in 9 years correlates very well. This technique unlike the previous two, is applicable to drilled pier as well as slab-on-grade foundations. Consideration of stress-void ratio relationships and final pore water pressure distributions are the major advantages of this technique and the good correlation bears this out.

6.5 Corps of Engineers. This method is very similar to McClelland and Sullivan's method with respect to the test procedure and analysis of the data. Consequently, the predictions should be very similar, and they are. No heave was predicted for the 25 ksf loadings while 0.41 inches of movement was predicted for the 2.7 ksf loadings. This correlates very well since these predictions assume the final pore water pressures equal zero which gives the largest heave prediction. This technique has all the advantages of McClelland and Sullivan's method as well as being able to predict settlement, so the overall movement of the structure can be assessed.

6.6 Computer Program HEAVE. Both modeling options, mechanical and suction, were used to predict heave under the MFSS. The results of each option will be discussed in separate paragraphs.

6.6.1 Mechanical Model. This model computes heave and consolidation using the Corps of Engineers technique. For the saturated profile a net settlement of 0.34 inches was predicted for pier H-18. Settlement occurred to a depth of 8 feet below the pier bottom while heave occurred in the remaining 12 feet of the active zone. Heave in the lower 12 feet amounted to 0.16 inch. Settlement of 1.58 inch was predicted using the hydrostatic profile for pier H-18. None of the soils below the pier heaved using this profile.

The prediction using the saturated profile correlates very well with the observed settlements under the 3 story portion of the MFSS which is where pier H-18 is located. The prediction using the hydrostatic profile does not correlate very well with the observed movements. Some of the discrepancy can be accounted for in time rate of settlement since the 1.58 inches is a total movement which will take a considerable amount of time to occur. Another factor to consider is that the hydrostatic profile assumes that the initial and final pore water pressures at the bottom of the active zone do not change. Properly selecting this pore water pressure will have a significant impact on the results. The value selected for these analyses was the average of the expansion pressure less the overburden pressure from the three

expansion-consolidation tests. This is the procedure McClelland and Sullivan used to select initial pore water pressures. This procedure seemed logical prior to performing the analyses and no other logical procedure for determining this parameter has been determined subsequent to these analyses. A better method for evaluating the pore water pressures is probably the only solution to obtaining more realistic solutions.

The program also computes the force at the bottom of the shaft which is equal to the load at the top less any load taken out in skin friction resulting from expansion of the soil adjacent to the shaft. A compressive load of 268 tons (536 kips) was predicted. The load measured in pier H-18 at gage 5 was 110 kips compression so the prediction is quite high. See Appendix C for detailed analysis of uplift force. If the program is underestimating the load taken out due to expansion of the soils adjacent to the pier shaft, inadequate tension steel may be placed in the shaft. This could result in tension failures in the pier shaft and excessive heave of the structure.

6.6.2 Suction Model. The results using the saturated profile were well in excess of what was measured. Three things should be considered when comparing this prediction with the observed movements. First is that the program assumes all of the heave occurs in the vertical direction while actually some will occur in the lateral direction. The prediction could be reduced by one-third to one-half to account for this since some of the expansion will occur laterally. Second the prediction is an

ultimate movement that may take decades to occur. Third, and most important, the assumption of a saturated profile is extremely conservative since it is unlikely to occur over the entire active zone. The soils immediately below the pier may become saturated to a depth of a few feet but these soils will form a barrier to the passage of water to the underlying soils. The main value of using this profile is to establish an upper limit of heave that might be expected.

The results using the Hydrostatic II profile were very satisfactory. Settlement was predicted for all three piers. The predicted movement was within the observed movements.

Loads at the bell using this model were the same as for the mechanical model and the same conclusions apply.

6.6.3 Conclusions. The suction model using the saturated profile should be used to provide an upper limit for the heave predictions. The suction model using the Hydrostatic II profile or the mechanical model with the saturated profile gave the best results compared to the observed movements. The mechanical model with Hydrostatic II profile predicted settlements in excess of those observed but this is most likely due to the accuracy of selecting the pore pressure at the bottom of the active zone as well as being a function of time rate of settlement.

## CHAPTER 7

### CONCLUSIONS

The following conclusions can be drawn from the comparisons made in the preceding chapter:

(1) The analysis techniques should be used to predict performance only for foundation types for which they were developed. Extending a technique data beyond the limits for which it was intended can lead to unconservative results. The techniques developed by van der Merwe and by Vijayvergia and Ghazzaly are good examples of techniques designed for slab-on-grade and in this study they proved to be inadequate for piers.

(2) The analysis techniques using consolidometer tests (mechanical models) correlated best with the observed movements. These methods can be applied at any depth for any foundation type making them very versatile. Selection of one technique over another would have to be made on the basis of personal preference, cost, and amount of information desired. The answers do not differ appreciably.

(3) The results using the program HEAVE were marginally satisfactory. The predictions bracketed the measured movements. Soil suction is a very good concept and will probably see increasing use in the future but selection of the final pore water pressure profile needs more refinement in order to improve the accuracy of the predictions.

(4) The load at the bottom of the shaft predicted by the program HEAVE may be higher than actually occurs. This could lead to unconservative steel design for the shaft and result in tension failures, or uplift forces underestimated by Equation 4.1. Results of Appendix C show that factor  $\alpha$  should be one or skin friction approaches soil shear strength when estimating uplift forces.

## CHAPTER 8

### RECOMMENDATIONS FOR FURTHER STUDY

In the course of using the analysis techniques and analyzing the instrumentation data a number of assumptions of varying significances were made. The significant items that deserve additional study are:

(1) The final pore water pressure distribution. The importance of this was stressed by the writers of every technique that considered it.

(2) The depth of the active zone.

(3) Effects of heave adjacent to the pier shaft. The program HEAVE addressed this but only in computing the load at the bottom of the shaft. If the shaft of pier F-19 is broken, as suspected, this is certainly the cause.

(4) Soil Suction - This deserves further attention so that a heave mechanism can be explained and utilized in analysis rather than using the consolidometer tests which are in essence a scale model that is extrapolated to the field conditions, normally with good results.

(5) Development of instrumentation with a long service life to measure stress in concrete. Creep of the concrete in the top of the piers caused considerable difficulty in interpreting the strain gage data. Measuring the stress/strain in the concrete and steel would eliminate this problem.

(6) Continued monitoring of the instrumentation on the MFSS.

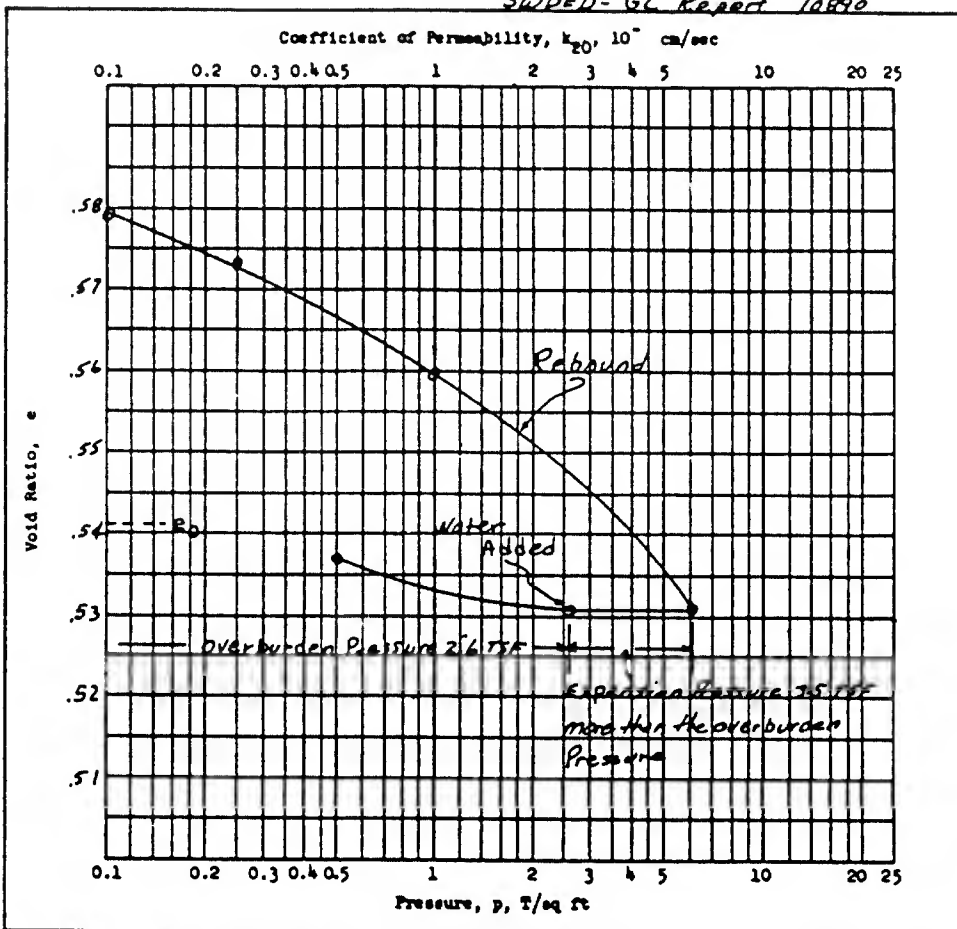
## REFERENCES

1. Statement of the Review Panel, Moisture Equilibria and Moisture Changes in Soils Beneath Covered Areas, G.D. Aitchison, ed., Butterworth, Sydney, Australia, p. 9
2. American Concrete Institute, Building Code Requirements for Reinforced Concrete (ACI 318-71), May 1976
3. Blight, G.E., "A Study of Effective Stress for Volume Change", Moisture Equilibria and Moisture Changes in Soils Beneath Covered Acres, Butterworth, Sydney, Australia, pp. 259-269
4. Headquarters, Department of the Army, "Correlation of Atterberg Limits and Consolidated Drained Shear Strength", Engineering Technical Letter No. 1110-1-58, 17 Feb 1972, Washington, D.C., pp. 1-2
5. Headquarters, Department of the Army, 1983, "Engineering and Design Foundations in Expansive Soils", TM 5-818-7, Washington, D.C.
6. Godfrey, K.A., Jr., "Expansive and Shrinking Soils-Building Design Problems Being Attacked," Civil Engineer, Vol. 48, No. 10, Oct 1978, pp. 87-91
7. Jobs, W.P. and Stroman, W.R., "Structures on Expansive Soils", Technical Report M-81, April 1974, Construction Engineering Research Laboratory, Champaign, Ill., p. 47
8. Jones, E., and Holtz, W., "Expansive Soils - The Hidden Disaster," Civil Engineering, Vol. 43, No. 8, Aug 1973, p. 49-51
9. Kantery, B., "Some secrets to building structures on expansive soils," Civil Engineering, Vol. 50, No. 12, Dec 1980, p. 53-55
10. van der Merwe, D.H., "The Prediction of Heave from the Plasticity Index and Percentage Clay Fraction of Soils", Civil Engineer in South Africa, Vol. 6, No. 6, June 1964, pp. 103-105
11. Mitchell, J.K., Fundamentals of Soils Behavior, 1st Edition, John Wiley & Sons, Inc., New York, 1976
12. Neville, A.M., Creep of Concrete: Plain, Reinforced, and Prestressed, 1st Edition, North-Holland Publishing Company, Amsterdam, 1970

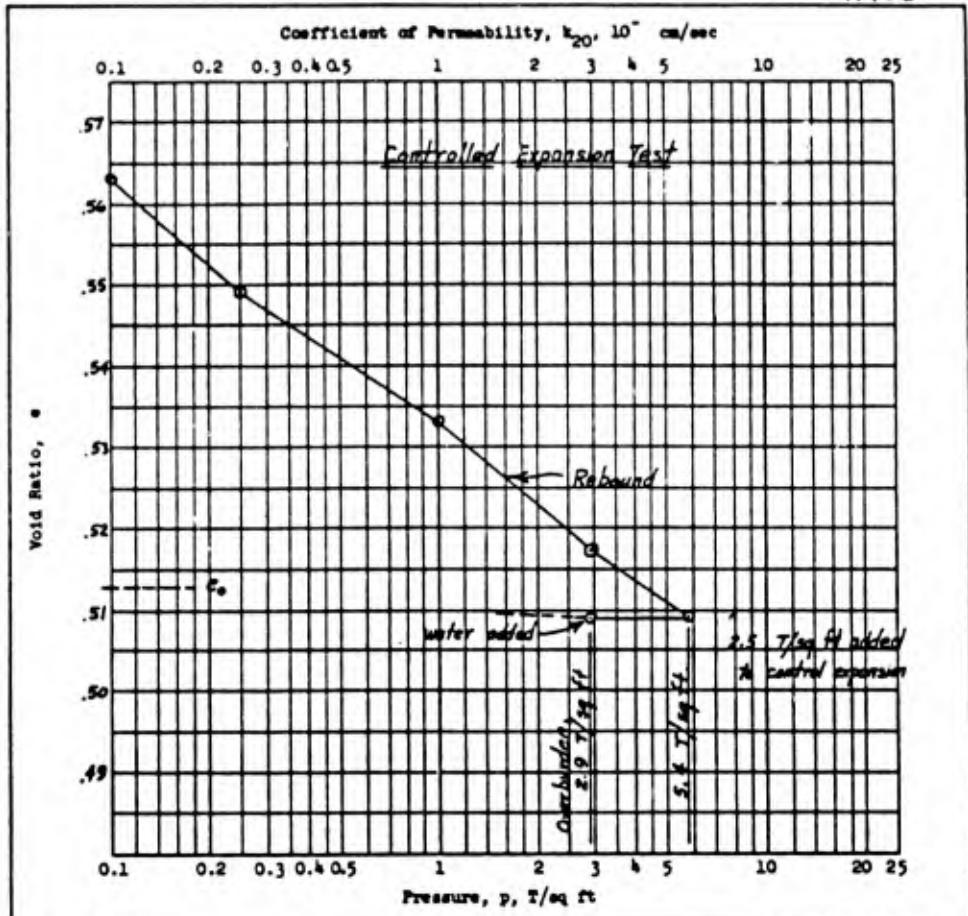
13. Sullivan, R.A. and McClelland, B., "Predicting Heave of Building on Unsaturated Clay", Proceedings of the Second International Research and Engineering Conference on Expansive Clay Soils, Texas A&M Press, 1969, pp. 404-420
14. Troxell, G.E., Davis, H.E., Kelly, J.W., Composition and Properties of Concrete, 2nd Edition, McGraw-Hill Book Company, New York, 1956, pp. 318-319
15. U.S. Army Engineer District, Fort Worth, "Investigations for Building Foundations in Expansive Clays", Volume 1 and 2, April 1968, Fort Worth, TX
16. Vijayvergia, V.N. and Ghazzaly, O.T., "Prediction of Swelling Potential for Natural Clays", Proceedings Third International Conference on Expansive Clay Soils, Vol. I, Haifa, Israel, 1973, pp. 227-234
17. White, W.A., "Atterberg Plastic Limits of Clay Minerals," American Mineralogist, Vol. 34, pp. 508-512
18. Yong, R.N. and Warkentin, B.P., "Volume Changes in Clay Soils," Introduction to Soil Behavior, 2nd Edition, The McMillan Co., New York, 1975, pp. 153-158

APPENDIX A

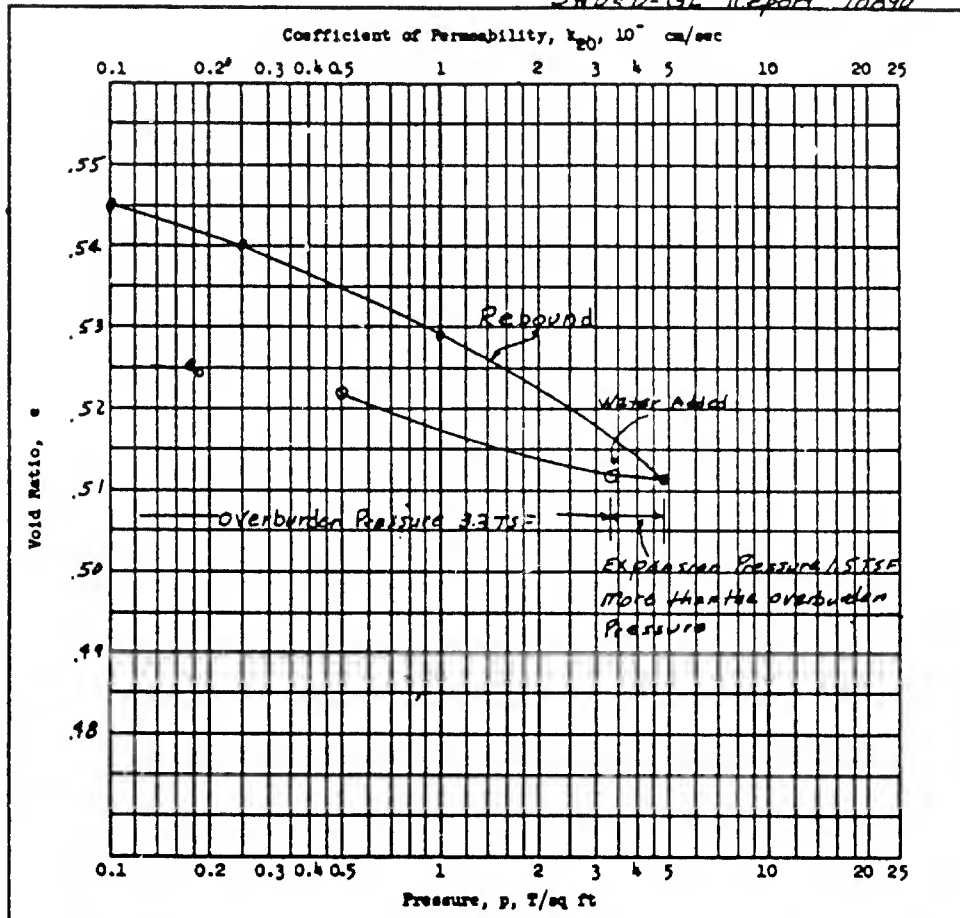
SWELL PRESSURE TEST RESULTS



Type of Specimen		Before Test		After Test	
Undisturbed					
Diam 4.44 in.	Ht 2H = 0.88 in.	Water Content, v <sub>0</sub>	18.8 %	v <sub>2</sub>	20.6 %
Overburden Pressure, P <sub>0</sub>	T/sq ft	Void Ratio, e <sub>0</sub>	0.541	e <sub>2</sub>	0.579
Preconsol. Pressure, P <sub>c</sub>	T/sq ft	Saturation, S <sub>0</sub>	95 %	S <sub>2</sub>	97 %
Compression Index, C <sub>c</sub>		Dry Density, γ <sub>d</sub>	110 lb/ft <sup>3</sup>		
Classification	CLAYEY SHALE	k <sub>20</sub> at e <sub>0</sub> =	x 10 <sup>-7</sup> cm/sec		
LL 59	U <sub>s</sub> 2.72 est	Project Fort Sam Houston			
PL 15	D <sub>10</sub>				
Remarks		Area			
		Boring No. BAK-187	Sample No. X-12211		
		Depth El 400-410	Date 22 Dec, 1969		
<b>CONSOLIDATION TEST REPORT</b>					



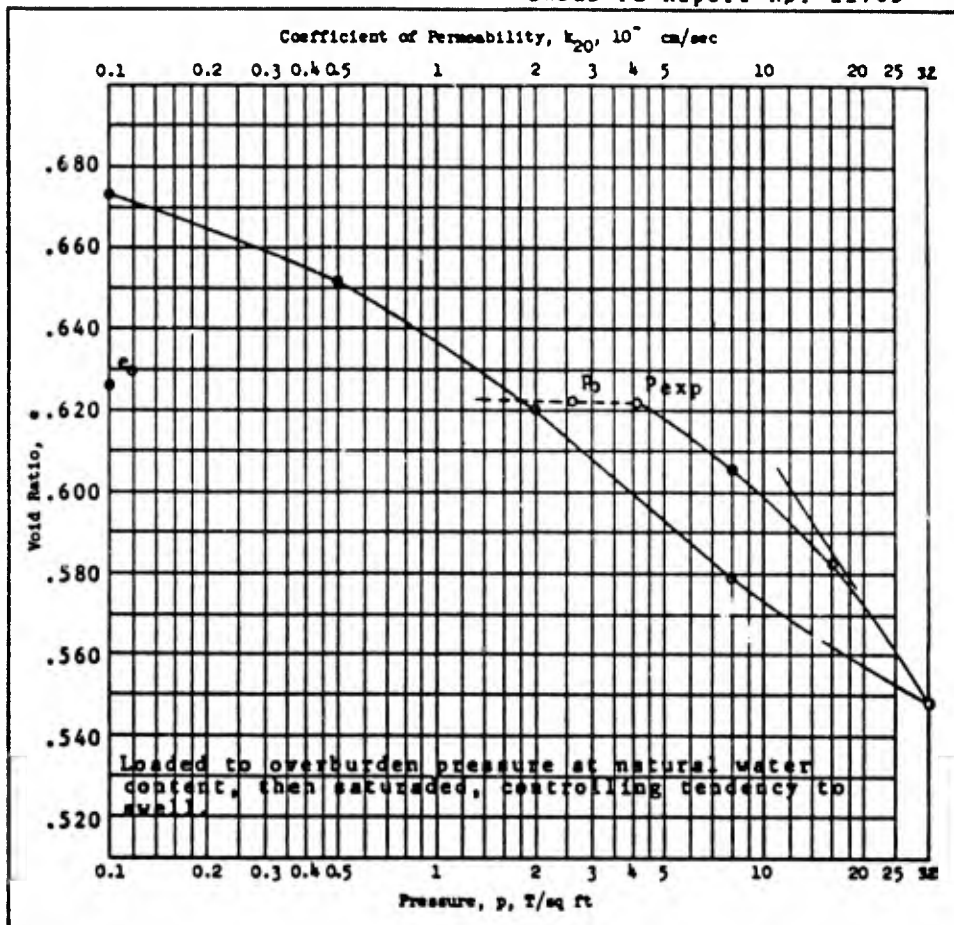
Type of Specimen		Before Test		After Test	
Diam 4.45 in.	Ht 2H = 0.89 in.	Water Content, $w_0$	18.7 %	$w_f$	21.2 %
Overburden Pres. $p_0$	2.9 T/sq ft	Void Ratio, $e_0$	.513	$e_f$	.563
Preconsol. Pressure, $p_c$	T/sq ft	Saturation, $S_0$	96 %	$S_f$	99 %
Compression Index, $C_c$		Dry Density, $\gamma_d$	109 lb/ft <sup>3</sup>		
Classification	CLAY SHALE	$k_{20}$ at $e_0 =$	x 10 <sup>-7</sup> cm/sec		
LL 71	$G_s$ 2.64	Project Fort Sam Houston			
PL 15	$D_{10}$				
Remarks Water content specimens dried at 140° F.		Area		(C-5)	
		Boring No. 8AGC-319 TP	Sample No. S-1683		
		Depth El 43.5 - 44.4	Date		
<b>CONSOLIDATION TEST REPORT</b>					



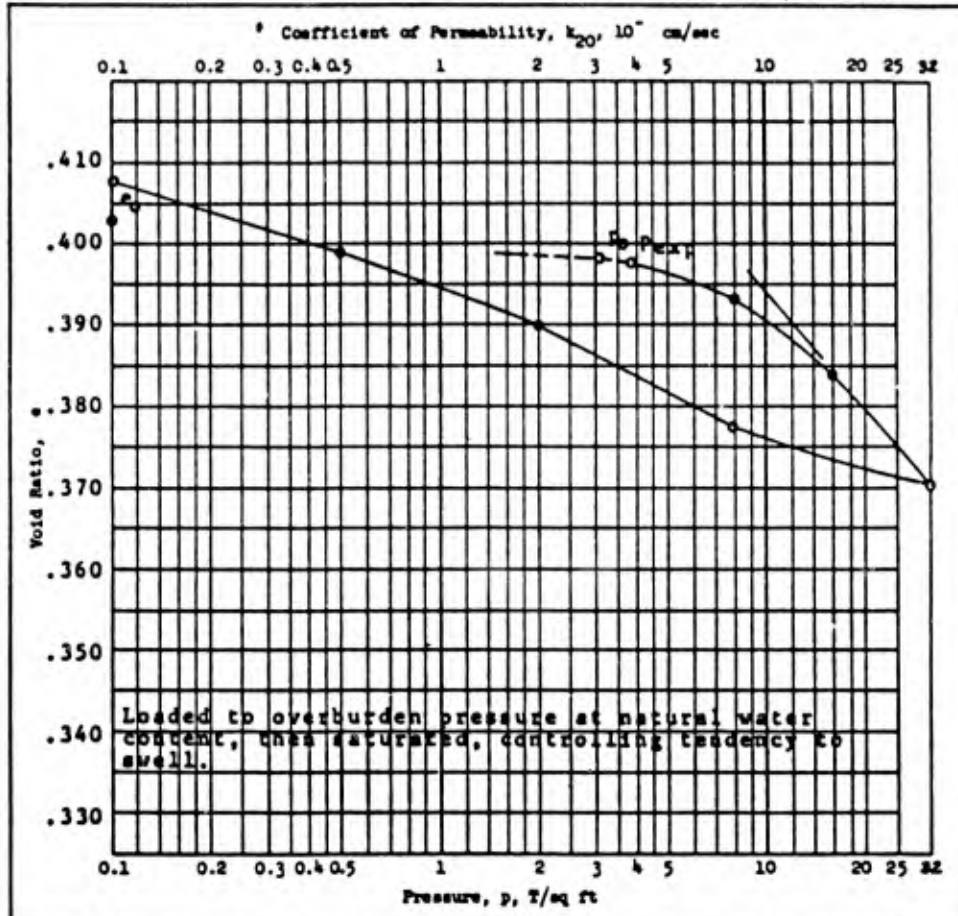
Type of Specimen		Before Test		After Test	
Undisturbed		Diam 4.45 in.	Ht 2H=0.88 in.	Water Content, $w_0$	17.6 %
				Void Ratio, $e_0$	0.525
				Saturation, $S_0$	91 %
				Dry Density, $\gamma_d$	111 lb/ft <sup>3</sup>
Classification CLAYEY SHALE		$k_{20}$ at $e_0 =$ x 10 <sup>-</sup> cm/sec			
LL 53	$U_c$ 272 est.	Project Fort Sam Houston			
PL 15	$D_{10}$	Area			
Remarks		Boring No. BAK-183		Sample No. X-12212	
		Depth El 500-510		Date 22 Dec 1969	
<b>CONSOLIDATION TEST REPORT</b>					

APPENDIX B

CONSOLIDATION-EXPANSION TEST RESULTS



Type of Specimen		Undisturbed		Before Test		After Test			
Diam	4.44 in.	Ht	.88 in.	Water Content, $w_o$	23.0 %	$w_r$	25.1 %		
Overburden Pressure, $P_o$	T/sq ft			Void Ratio, $e_o$	.626	$e_r$	.673		
Preconsol. Pressure, $P_c$	T/sq ft			Saturation, $S_o$	98 %	$S_r$	99 %		
Compression Index, $C_c$	0.12			Dry Density, $\gamma_d$	102.8 lb/ft <sup>3</sup>				
Classification	CLAY SHALE			$k_{20}$ at $e_o =$	$\times 10^{-7}$ cm/sec				
LL	85	$U_c$	2.68	Project				Fort Sam Houston	
FL	18	$D_{10}$		Area				(C-3)	
Remarks				Boring No.		8A6C-345		Sample No.	S-1456
				Depth		El 38.8-39.7		Date	
<b>CONSOLIDATION TEST REPORT</b>									



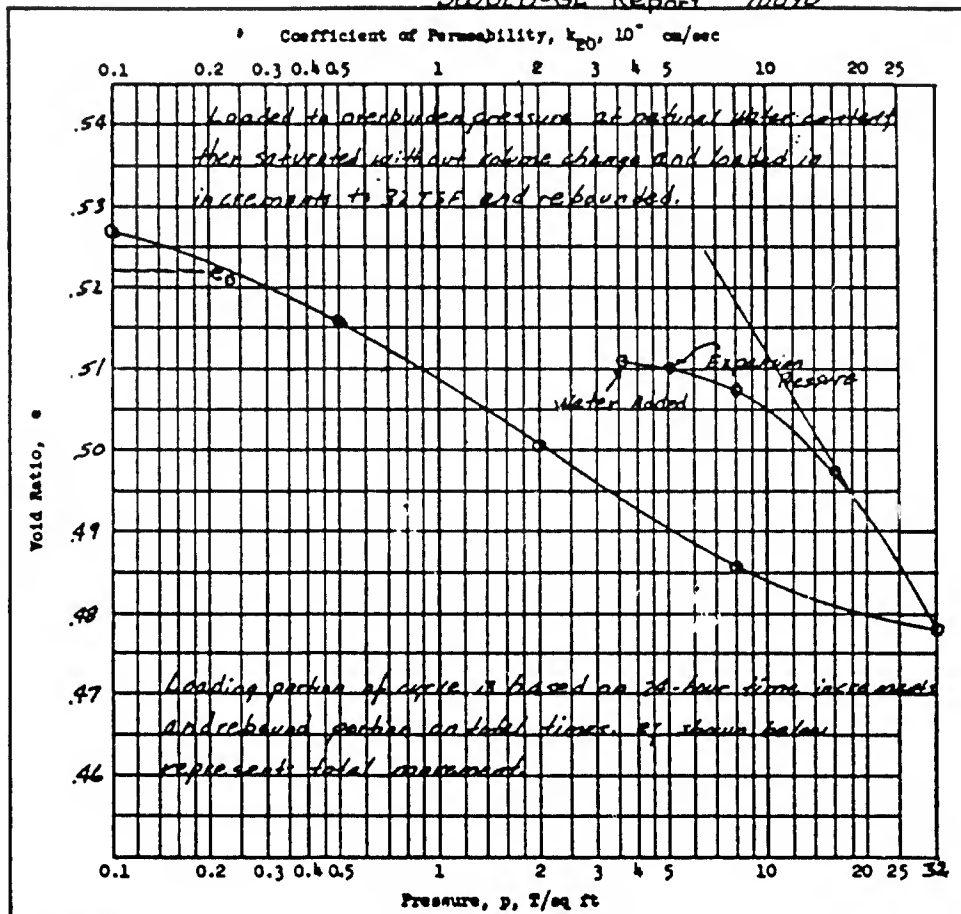
Type of Specimen Undisturbed		Before Test		After Test	
Diam 4.44 in.	Ht .88 in.	Water Content, $w_o$	15.5 %	$w_f$	16.6 %
Overburden Pressure, $P_o$	T/sq ft	Void Ratio, $e_o$	.402	$e_f$	.407
Preconsol. Pressure, $P_c$	T/sq ft	Saturation, $S_o$	100 %	$S_f$	105 %
Compression Index, $C_c$	0.05	Dry Density, $\gamma_d$	115.7 lb/ft <sup>3</sup>		
Classification	CLAY SHALE	$k_{20}$ at $e_o =$	$\times 10^{-7}$ cm/sec		
LL	59	$G_s$	2.60		
FL	15	$D_{10}$			
Remarks	Area (C-4)				
	Boring No. 8A6C-354		Sample No. S-1384		
	Depth El 47.9-48.9		Date Sept. 73		
<b>CONSOLIDATION TEST REPORT</b>					

DDG FORM 2090  
1 MAY 68

PREVIOUS EDITIONS ARE OBSOLETE. (THRU) (PERCENT)

1 4 2 4

SWDED-GL Report 10890



Type of Specimen		Before Test		After Test	
Undisturbed					
Diam 4.45 in.	$e_c^{2H^a}$ 0.88 in.	Water Content, $w_o$	17.7 %	$w_r$	18.9 %
Overburden Pressure, $P_o$	T/eq ft	Void Ratio, $e_o$	.522	$e_r$	.526
Preconsol. Pressure, $P_c$	T/eq ft	Saturation, $S_o$	91 %	$S_r$	97 %
Compression Index, $C_c$	0.07	Dry Density, $\gamma_d$	111 lb/ft <sup>3</sup>		
Classification CLAYEY SHALE		$k_{20}$ at $e_o =$ x $10^{-7}$ cm/sec			
LL 53	$U_o$ 2.69	Project Fort Sam Houston			
PL 14	$D_{10}$				
Remarks		Area			
		Boring No. BAK-183	Sample No. X-12213		
		Depth El 55.7-56.7	Date 22 December 1962		
<b>CONSOLIDATION TEST REPORT</b>					

ENG FORM 2090  
1 MAY 55

PREVIOUS EDITIONS ARE OBSOLETE. (TRANSPARENT)

0 8424

APPENDIX C  
COMPUTATION OF UPLIFT FORCES ON  
DRILLED PIER SHAFT

C.1 General.- One of the conclusions reached in Chapter 7 was that the computer program HEAVE overpredicts the load at the bottom of the pier. The program computes this load by subtracting the computed uplift load from the input column load. Since column loads can be fairly accurately determined any discrepancy should lie in computing the uplift load.

The program currently computes uplift using the following equation:

$$Q_u = \sum_0^L (P_{exp} - P_o) A_{act} \cdot \alpha \leq \sum_0^L (P_o \tan \phi + c) A_{act} \cdot \alpha$$

where

$Q_u$  = Uplift force

$L$  = Length of pier in active zone

$P_{exp}$  = Expansion pressure

$P_o$  = Overburden pressure

$A_{act}$  = Area of pier shaft increment =  $\pi \cdot D_s \cdot l$

$D_s$  = Shaft diameter

$l$  = Shaft increment length

$\alpha$  = Skin friction reduction factor

$\phi$  = Soil friction angle

$c$  = Soil cohesion

This equation represents the two logical approaches that can be used to compute uplift. Either that portion of the expansion pressure in excess of overburden pressure or the soil-shaft skin friction (determined from shear strength) is multiplied by the surface area of the pier the expansive soil reacts against and modified by a skin friction reduction factor. The skin friction reduction factor is normally assumed to be 1.0, for conservatism, rather than the 0.3 to 0.4 used when designing for load

carrying capacity. A value of 1.0 has been used in all of the computations for this appendix. The accuracy of the uplift computation is primarily dependent on the values selected for expansion pressure, soil friction angle and soil cohesion. Selection of these parameters and which of the approaches, excess expansion pressure or skin friction, produces more credible results will be discussed in the remainder of this appendix.

C.2 Computation of Uplift.- Four approaches to selecting design parameters will be presented, two for expansion pressure and two for skin friction.

C.2.1 General.- Uplift forces will be computed for piers H-16 and H-18 down to a depth of 28 feet below the ground surface. Strain gages H-16-5 and H-18-5 are located at this depth and will provide a means of comparing the predicted loads with currently existing loads. The actual uplift force will be computed using two column loads, the design column load and the load currently at the uppermost strain gage, H-16-1 and H-18-1. All of this information is shown in the following table. All values are in tons.

MEASURED UPLIFT FORCES

<u>Pier</u>	<u>Load at 28 Feet</u>	<u>Design Col. Load</u>	<u>Design Uplift</u>	<u>Current Col. Load</u>	<u>Current Uplift</u>
H-16	210	497	287	827	617
H-18	57	481	424	415	358

Each of the four approaches will be discussed in the following paragraphs. A summary will be presented at the end.

C.2.2 Case 1.- The simplest approach is to take the expansion pressure directly from laboratory test results. Using this approach uplift of 309 tons and 258 tons were computed for piers H-16 and H-18 respectively.

C.2.3 Case 2.- An alternative to Case 1 is to use the Casagrande construction<sup>(1)</sup> which will provide an estimate of the maximum past pressure, i.e., a larger value of expansion pressure. Uplifts of 893 tons and 746 tons for piers H-16 and H-18 respectively were computed.

C.2.4 Case 3.- The simplest skin friction approach is to use undrained (Q) strength test results and assume  $\phi$  equals zero. Since 1-point Q-triaxial tests and unconfined compression tests normally comprise the majority of strength testing for building foundation design, this information is normally available as part of the routine testing program. Using this approach, uplifts of 471 tons and 394 tons were computed for piers H-16 and H-18 respectively.

C.2.5 Case 4.- This final method involves using the equation presented in paragraph 4.1.4 which uses results from direct shear tests. Uplift forces of 306 tons and 255 tons were computed for piers H-16 and H-18 respectively.

C.2.6 Summary.- The computed uplifts are summarized in the following table. All values are in tons.

COMPUTED UPLIFT FORCES

<u>Pier</u>	<u>Case 1</u>	<u>Case 2</u>	<u>Case 3</u>	<u>Case 4</u>	<u>Measured</u>
H-16	309	893	471	306	617
H-18	258	746	394	255	358

In order to compare the above computed values with the measured uplift forces, the computed values are expressed as a percentage of the two measured values discussed earlier in the following table.

COMPUTED UPLIFT AS A PERCENTAGE OF MEASURED UPLIFT

Pier	Case 1		Case 2		Case 3		Case 4	
	Design	Current	Design	Current	Design	Current	Design	Current
H-16	108	50	311	145	164	76	107	50
H-18	61	72	176	209	93	110	60	71

C.3 Conclusions.- Based on the preceding table, the following conclusions can be reached.

1. Case 3 correlated the closest to the measured uplift forces.
2. Cases 1 and 4 gave almost the same answers despite one using the excess expansion pressure approach and the other using the skin friction approach.
3. Cases 1 and 4 correlated fairly well though they tended to under predict the uplift and are therefore somewhat unconservative.
4. Case 2 over predicted the uplift by a significant margin. Since the measured uplift is based on only 9 years of observations, total uplift along the full length of the pier shaft may not have developed yet. This would explain the apparent over prediction. Assuming full uplift has developed, this approach would provide a factor of safety of 1.5 to 2.0 against failure of the pier shaft in tension, assuming adequate reinforcing steel is provided in the pier shaft.

C.4 Recommendations.- Based on the preceding conclusions, the following recommendations are made.

Uplift forces computed using any of the four cases presented should be carefully evaluated using engineering judgement, experience in the

same area and performance of similar structures in similar conditions. The last item should be given particular emphasis. If a particular design approach has performed successfully, it should not be changed without good reason. For structures that are sensitive to movement or of a critical nature, where a conservative design can be justified, Case 2 is recommended. This case will predict the maximum uplift and should provide some factor of safety.

Structures that are less critical and can tolerate some movement can be designed using Case 3. This case appears to provide little or no factor of safety, consequently Cases 1 and/or 4 should be used to check the results of Case 3.

All of these approaches should be used with caution. The predictions can vary considerably from what is observed, both on the conservative and unconservative side. Continued observations at the MFSS and other projects of a similar nature are the best means to update and refine the analysis techniques available.

#### REFERENCES

1. Terzaghi, K. and Peck, R.B., Soil Mechanics in Engineering Practice, 2nd edition, John Wiley & Sons, Inc., New York, 1967, pg 77.